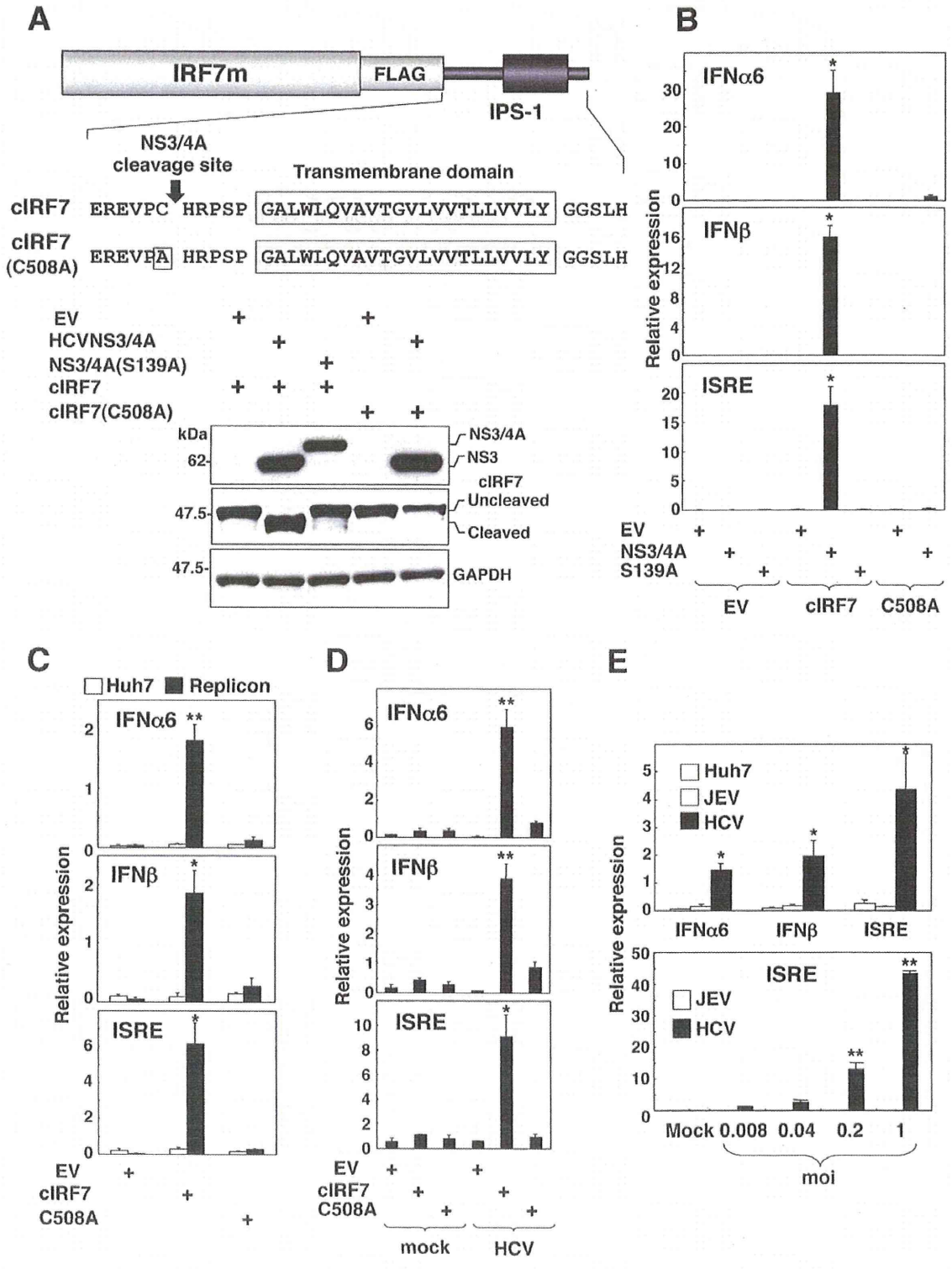

Figure 2. Construction of cIRF7 capable of activating the IFN promoters in cells replicating HCV. (A top) Schematic representation of the cIRF7 constructs. cIRF7 consists of IRF7m, FLAG-tag, and IPS-1 (503 to 540 amino acid residues) sequences containing a cleavage site by HCV NS3/4A protease, a transmembrane domain and a cytoplasmic region modified to localize on the ER. cIRF7(C508A) has a substitution of Cys508 to Ala which renders it resistant to the cleavage by the HCV protease. (A bottom) Immunoblot analyses of 293T cells transfected with a plasmid encoding either cIRF7 or cIRF7(C508A) together with either an empty vector (EV) or a plasmid encoding either FLAG-tagged HCVNS3/4A or FLAG-tagged HCVNS3/4A (S139A). (B) 293T cells (2×10^5 cells/well) were transfected with a plasmid of EV, FLAG-tagged HCVNS3/4A or FLAG-tagged HCVNS3/4A(S139A) in combination with a plasmid of EV, cIRF7 or cIRF7 (C508A) together with 100 ng of the reporter plasmid encoding the luciferase gene under the

control of the IFNα6, IFNβ or ISRE promoter, and luciferase activity was determined at 24 h post-transfection. (C) HCV replicon cells (1.5×10^5 cells/well) and (D) Huh7OK1 cells (7.5×10^4 cells/well) infected with HCVcc at an moi of 1 and incubated for 72 h were transfected with 100 ng of each of the reporter plasmids together with plasmid of EV, cIRF7 or cIRF7(C508A) and luciferase activity was determined at 24 h post-transfection. (E) Huh7 cells, HCV subgenomic replicon cells, and JEV subgenomic replicon cells (1×10^5 cells/well) (top) and Huh7OK1 cells (7.5×10^4 cells/well) infected with JEV and HCV (bottom) at an moi of 0.008, 0.04, 0.2, and 1 and incubated for 24 h and 72 h, respectively, were transfected with 100 ng of each of the reporter plasmids together with cIRF7 and the luciferase activity was determined at 24 h post-transfection. The data shown in this figure are representative of three independent experiments. The error bars represent the standard deviations. Asterisks indicate significant differences (*$P<0.05$, **$P<0.01$) versus the control cells or mock-infected cells.
doi:10.1371/journal.pone.0015967.g002

replicating HCV. To tightly regulate activation of the molecules in HCV- infected cells, we employed the C-terminal amino acid sequence of human IPS-1, which has been identified as an adaptor molecule involved in the RIG-like receptor (RLR) signaling pathways. It has been demonstrated that HCV NS3/4A protease efficiently cleaves the upstream position of the transmembrane region of IPS-1 on the mitochondrial outer membrane and disrupts the IFN signaling pathway [15–18]. Furthermore, to avoid induction of mitochondrial dysfunction and cell death due to the expression of the therapeutic molecules on the mitochondria, we replaced three arginine residues among the C-terminal five residues of IPS-1 with non-charged amino acid glycine residues (RRRLH to GGGLH) so that these three residues would be localized on the ER membrane [21]. HCV is suggested to replicate on the ER membrane, and therefore subcellular localization and distance of the cleavage site of the substrates from the membrane could be crucial for an efficient processing. The tightly regulated activation of the therapeutic molecules in cells replicating HCV observed in this study might be largely attributable to the ER localization of the therapeutic molecules.

Irrespective of IFN sensitivity, the expression of cIRF7 in the HCV replicon cells induced the activation of type I IFN promoter and inhibited the viral RNA replication, suggesting the possibility that cIRF7 could be used for the treatment of hepatitis C patients who are infected with HCV resistant to IFNα therapy. The expression of IRF3m in cells infected with HCVcc induced a higher antiviral response than that in the Con1 replicon cells in spite of the comparable transcription of IFNβ mRNA between the two cell types Fig. 1), suggesting that differences among HCV genotypes might be caused to the difference to the sensitivity of IFNβ. To assess the real efficacy of cIRF7 for suppression of HCV replication, we must await the establishment of robust cell culture systems capable of propagating various genotypes of HCV derived from the sera of hepatitis C patients.

It has been shown previously that HCV interferes with the induction of type I IFN through the cleavage of IPS-1 by NS3/4A protease [15–18], the interaction of NS5A with MyD88, a major adaptor molecule of TLRs [33], and the intervention of the IFNα-activated Jak-STAT signaling pathway by HCV proteins [7–9]. After cleavage by the HCV protease, the processed cIRF7 migrates into the nucleus and activates various IFN promoters, and it may participate in regulation of the expression of hundreds of ISGs, suggesting that cIRF7 is capable of inducing an antiviral response through the Jak-STAT-independent pathway. Although it has been reported previously that the basal expression of IRF7 and the IRF7-induced activation of the IFNα promoter are impaired in the HCV replicon cells [34], in this study we have shown that cIRF7 is activated in cells infected with HCVcc and capable of inducing type I IFN. Collectively, these results suggest that cIRF7 is capable of eliminating HCV that persistently infects

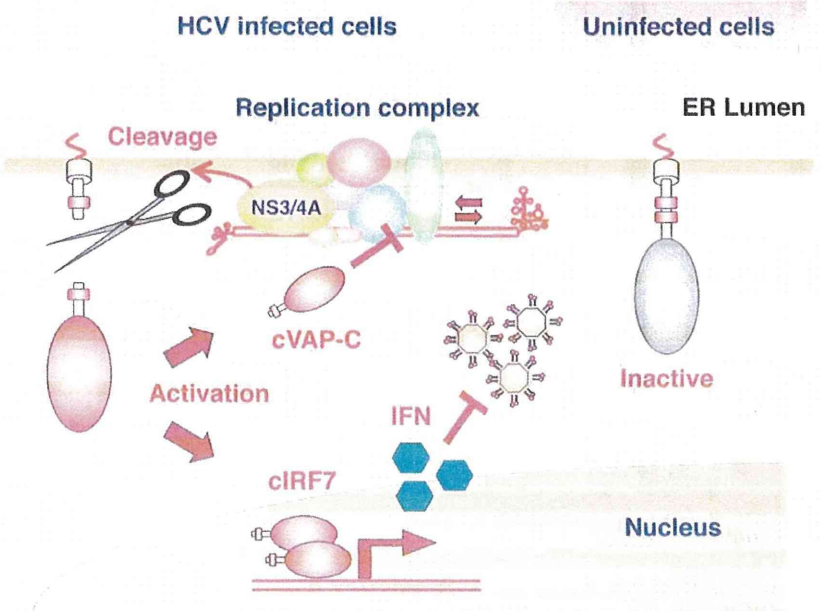

Figure 3. Scheme of activation of the therapeutic molecule in cells infected with HCV. The chimeric molecules are cleaved by HCV NS3/4A protease and the released fragments inhibit propagation of HCV through induction of IFN after translocation into the nucleus (cIRF7) or disruption of the replication complex (cVAP-C), whereas the molecule is stably anchored in the ER within uninfected cells.
doi:10.1371/journal.pone.0015967.g003

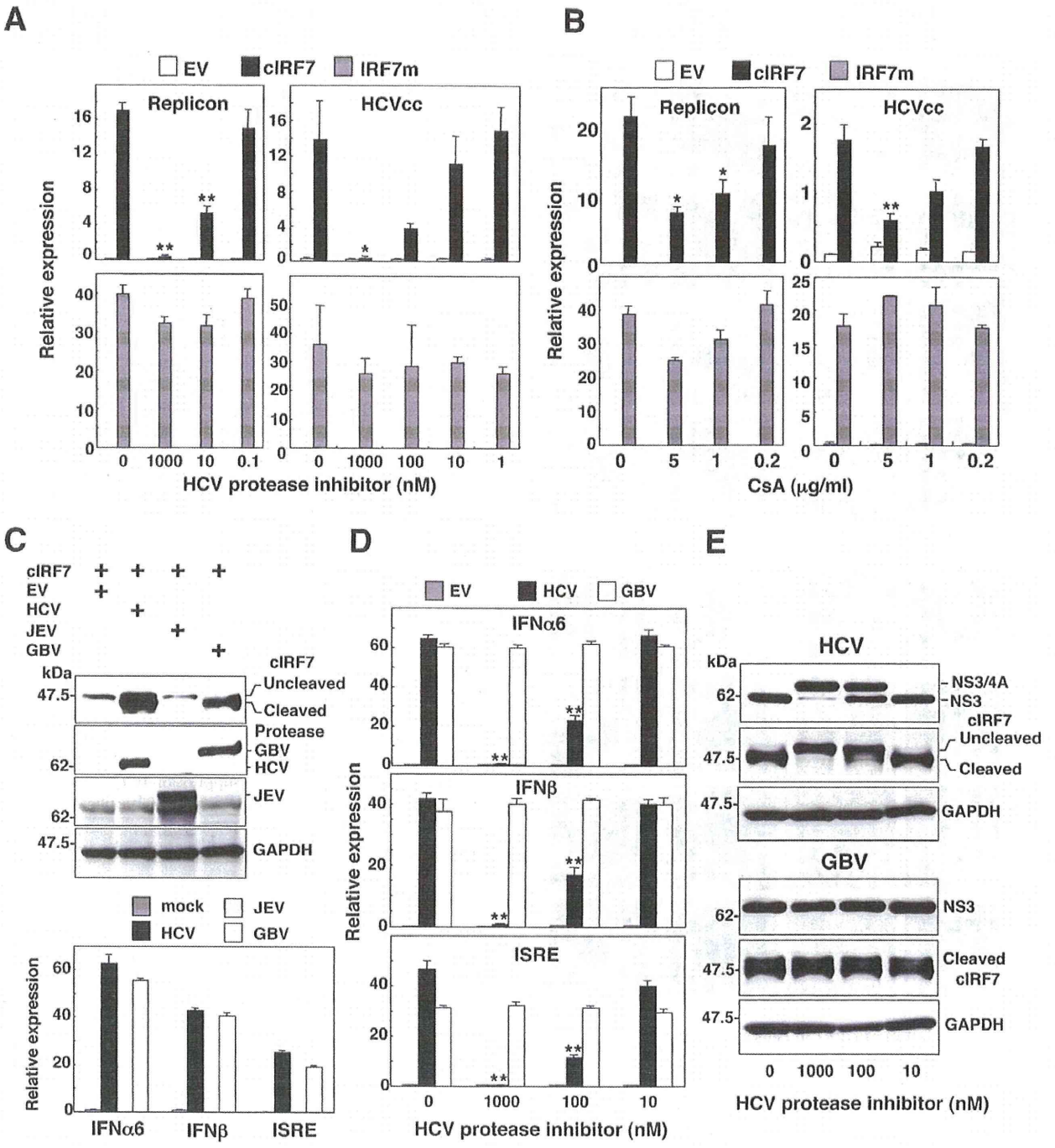

Figure 4. Specificity of activation of the IFN promoters by the expression of cIRF7. (A) HCV replicon cells (1.5×10^5 cells/well) or Huh7OK1 cells (7.5×10^4 cells/well) infected with HCVcc at an moi of 1 and incubated for 72 h were treated with various concentrations of HCV protease inhibitor (A) or cyclosporine A (CsA) (B), transfected with an empty vector (EV) (white bars) or plasmids encoding cIRF7 (black bars) or IRF7m (gray bars) together with 100 ng of a reporter plasmid encoding the luciferase gene under the control of the ISRE promoter, and luciferase activity was determined at 24 h post-transfection. (C top) A plasmid encoding cIRF7 was co-transfected with a plasmid encoding either FLAG-tagged HCVNS3/4A, FLAG-tagged GBVNS3/4A, or HA-tagged JEVNS2b/3 into 293T cells, and the expressions of cIRF7, viral proteases and GAPDH were determined by immunoblotting. (C bottom) 293T cells (2×10^5 cells/well) transfected with a plasmid encoding either EV (dark gray bars), FLAG-tagged HCVNS3/4A (black bars), FLAG-tagged GBVNS3/4A (white bars), or HA-tagged JEVNS2b/3 (gray bars) together with 100 ng of the plasmid encoding the luciferase gene under the control of the promoter of either IFNα6, IFNβ or ISRE, and luciferase activity was determined at 24 h post-transfection. (D) 293T cells (2×10^5 cells/well) were transfected with 100 ng of the reporter plasmids together with plasmids encoding EV (gray bars), FLAG-tagged HCVNS3/4A (black bars) or FLAG-tagged GBVNS3/4A (white bars) in the presence or absence of the HCV protease inhibitor, and luciferase activity was determined at 24 h post-transfection. (E) cIRF7 was co-expressed with FLAG-tagged HCVNS3/4A or FLAG-tagged GBVNS3/4A in 293T cells in the presence or absence of the HCV protease inhibitor, and the expressions of cIRF7, viral proteases and GAPDH were determined by immunoblotting. The data shown in this figure are representative of three independent experiments. The error bars represent the standard deviations. Asterisks indicate significant differences (*$P<0.05$, **$P<0.01$) versus the control cells or mock-infected cells.
doi:10.1371/journal.pone.0015967.g004

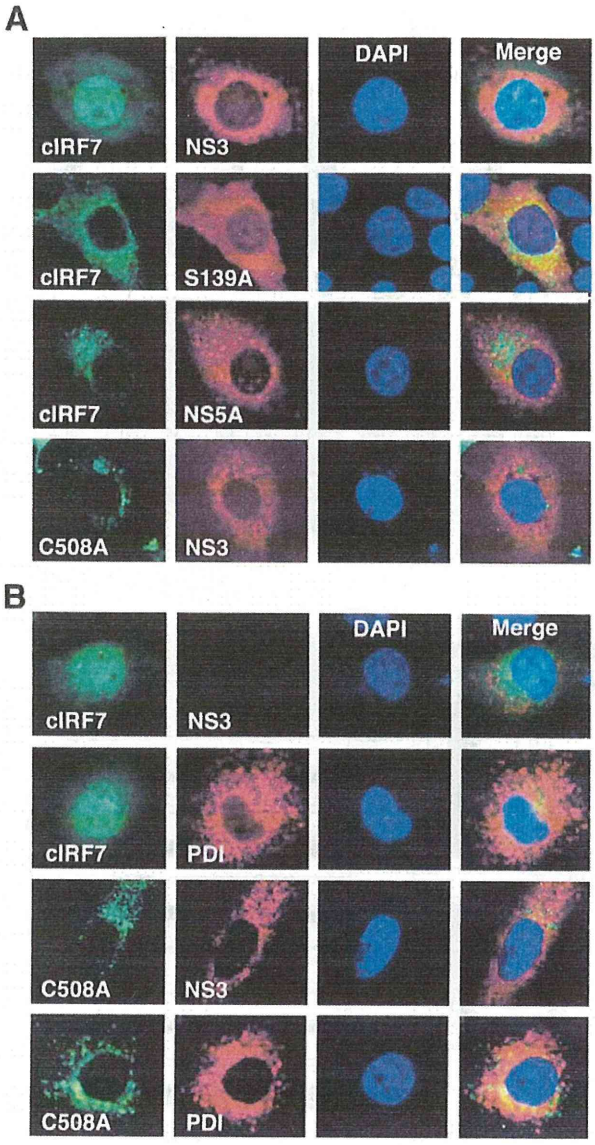

Figure 5. Activation of cIRF7 in cells expressing HCV protease. (A) Huh7OK1 cells (5×10^4 cells/well) were co-transfected with plasmids encoding either EGFP-cIRF7 or EGFP-cIRF7(C508A) and plasmids encoding either HCVNS3/4A, HCVNS3/4A(S139A) or NS5A, harvested at 24 h post-transfection, fixed with 4% paraformaldehyde in PBS, and permeabilized with 0.25% saponin. HCV NS3 and NS5A were stained with the appropriate antibodies, followed by staining with AF594-conjugated second antibodies. (B) HCV replicon cells (5×10^4 cells/well) were transfected with plasmids encoding either EGFP-cIRF7 or EGFP-cIRF7(C508A), and endogenous expression of HCV NS3 and an ER marker, PDI, was detected in cells treated and stained with the appropriate antibodies as described above. Subcellular localization of cIRF7s, HCV proteins and PDI was determined by confocal microscopy after staining of nuclei by DAPI. The data shown in this figure are representative of three independent experiments.
doi:10.1371/journal.pone.0015967.g005

human hepatocytes through an induction of sufficient amounts of type I IFN.

It is well known that patients achieving a rapid viral clearance by the treatment with PEG-IFNα showed a significant up-regulation of ISG, whereas a high level expression of ISG is observed in nonresponsive patients before IFN therapy, probably due to a rapid induction of negative regulators for the IFN signaling pathway, such as the suppressor of cytokine signaling proteins [35,36]. These results suggest that chronic hepatitis C patients with a pre-activated IFN signaling pathway respond poorly to IFN therapy. In this study we also demonstrated that activation of various IFN promoters by the expression of the dominant active mutants of IRFs was more accentuated in cells replicating HCV rather than naïve cells, probably due to an undetectable expression of ISG in cells replicating HCV RNA as described previously [37]. However, the precise mechanisms underlying the enhancement of IFN activity by the expression of a dominant active mutant of IRFs in cells replicating HCV remain unknown. Fillipowicz *et al.* suggested the possibility of recovery of the sensitivity to IFN therapy by the restoration of the endogenous IFN system to a "naïve" state through a blockage of the IFN response in nonresponders before treatment [36]. However, modulation of ISG expression before IFN therapy may induce a flare of HCV propagation in the liver of chronic hepatitis C patients. Therefore, it might be interesting to examine whether an effectiveness of cIRF7 are sustained in a state of occurring a negative regulator for IFN signaling pathway and preactivated IFN signaling pathway in cells replicating HCV.

VAP-A and VAP-B are suggested to be involved in the construction of the HCV replication complex consisting of viral proteins and host cellular lipid components, and that VAP-C interrupts the VAP-A and VAP-B functions and negatively regulates the HCV propagation and not expressed in human hepatocytes probably involves in the determination of tissue tropism of HCV [20]. Although further studies will be needed to elucidate the effectiveness of the molecules *in vivo* experiment using drug delivery systems including viral and non-viral vectors in more detail, therapeutic molecules consisting of host factors involved in IFN induction such as IRF7 and in the suppression of HCV replication such as VAP-C fused with the IPS-1 sequences specifically cleaved by the HCV protease might be a promising approach capable of eliminating HCV without induction of severe cellular toxicity.

Materials and Methods

Cells and viruses

Vero and 293T cell lines were purchased from American Type Culture Collection (Manassas, VA). Huh7 cell line was kindly provided by Ralf Bartenschlager. Huh7OK1 cell line was previously established from interferone-treated Huh7 cells including HCV replicon and exhibited high susceptibility to HCVcc propagation [38]. These cell lines were maintained in Dulbecco's modified Eagle's medium (DMEM) (Sigma, St. Louis, MO) supplemented with 10% fetal calf serum (FCS). Huh-9–13 cells harboring an HCV subgenomic RNA replicon of genotype 1b [39] were cultured in DMEM supplemented with 10% FCS, 1 mg/ml G418 and nonessential amino acids. The infectious RNA of the JFH1 strain was introduced into Huh7OK1 cells and the infectious titers were expressed as focus-forming units (FFU) [4]. Huh7 cells harboring a JEV subgenomic RNA replicon (Nakayama strain) were cultured in DMEM supplemented with 10% FCS and 1 μg/ml puromycin. Preparation of the HCV subgenomic replicon cells 4βR exhibiting an IFN-resistant phenotype and their cured cells 4βRc were described previously [27,28]. All cells were cultured at 37°C in a humidified atmosphere with 5% CO_2.

Plasmids and reagents

The cDNA fragments encoding IRF3 and IRF7 were amplified by PCR from a total RNA from THP-1 cells and cloned into

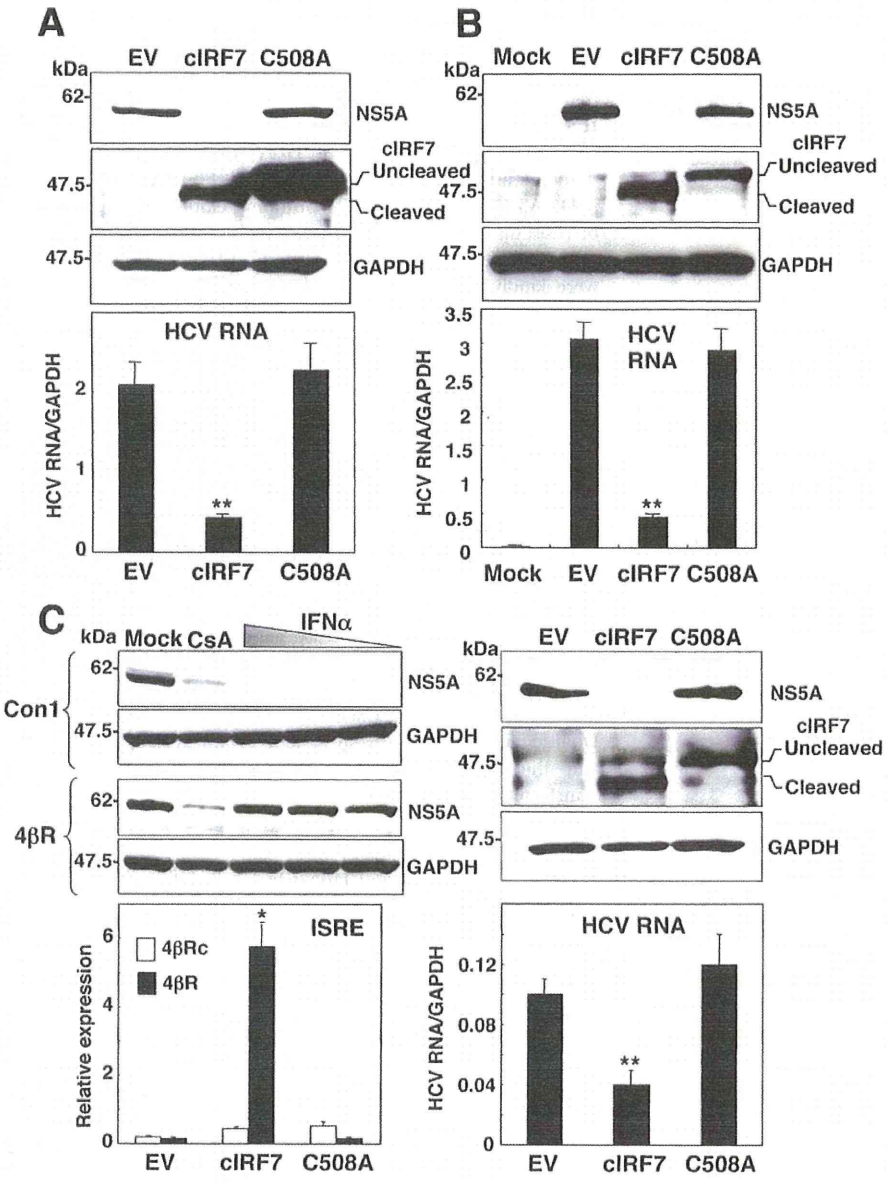

Figure 6. Suppression of HCV replication by the expression of cIRF7. (A) HCV replicon cells (3×10^5 cells/well) and (B) Huh7OK1 cells (1.5×10^5 cells/well) infected with HCVcc at an moi of 1 and incubated for 72 h were transfected with a plasmid encoding either empty vector (EV), cIRF7 or cIRF7(C508A), and the expression of NS5A, cIRF7s and GAPDH (upper panels) and synthesis of viral RNA (lower panels) were determined at 72 h post-transfection by immunoblotting and real-time PCR, respectively. (C upper left) HCV Con1 replicon cells and 4βR replicon cells exhibiting an IFN-resistant phenotype (1.5×10^5 cells/well) were treated with the CsA (5 μg/ml) or 10^4, 10^3, and 10^2 units/ml of recombinant human IFNα and the expressions of NS5A and GAPDH were determined by immunoblotting. The 4βR replicon cells (3×10^5 cells/well) were transfected with EV or plasmid encoding either cIRF7 or cIRF7(C508A), and the expressions of NS5A, cIRF7s and GAPDH (C upper right) and synthesis of viral RNA (C lower right) were determined at 72 h post-transfection by immunoblotting and real-time PCR, respectively. The 4βR cells and their cured cells (4βRc) with the HCV genome eliminated (1×10^5 cells/well) were transfected with EV or plasmid encoding either cIRF7 or cIRF7(C508A) together with 100 ng of plasmid encoding the luciferase gene under the control of the ISRE promoter, and luciferase activity was determined at 24 h post-transfection (C lower left). The data shown in this figure are representative of three independent experiments. The error bars represent the standard deviations. Asterisks indicate significant differences (*$P<0.05$, **$P<0.01$) versus the control cells or mock-infected cells.
doi:10.1371/journal.pone.0015967.g006

pcDNA3.1-C-myc-His (Invitrogen, Carlsbad, CA). The mutants carrying a deletion in the auto-inhibitory domain (from amino acid residue 284 to 454) of IRF7 and the substitution of Ser^{396} with phosphomimetic Asp located in the carboxyl terminus of IRF3 were generated by the method of splicing by overlap extension and cloning into pcDNA3.1myc-His and designated as IRF7m and IRF3m, respectively. N-terminally FLAG-tagged wild-type NS3/4A protease and its mutant substituted with Ser^{139} to replaced with Ala (S139A) were prepared as described previously [33]. The cDNA fragment encoding a JEV protease was amplified from a total RNA of Vero cells infected with JEV (AT31 strain) and cloned into pcDNA3.1Flag/HA [40], The cDNA fragment

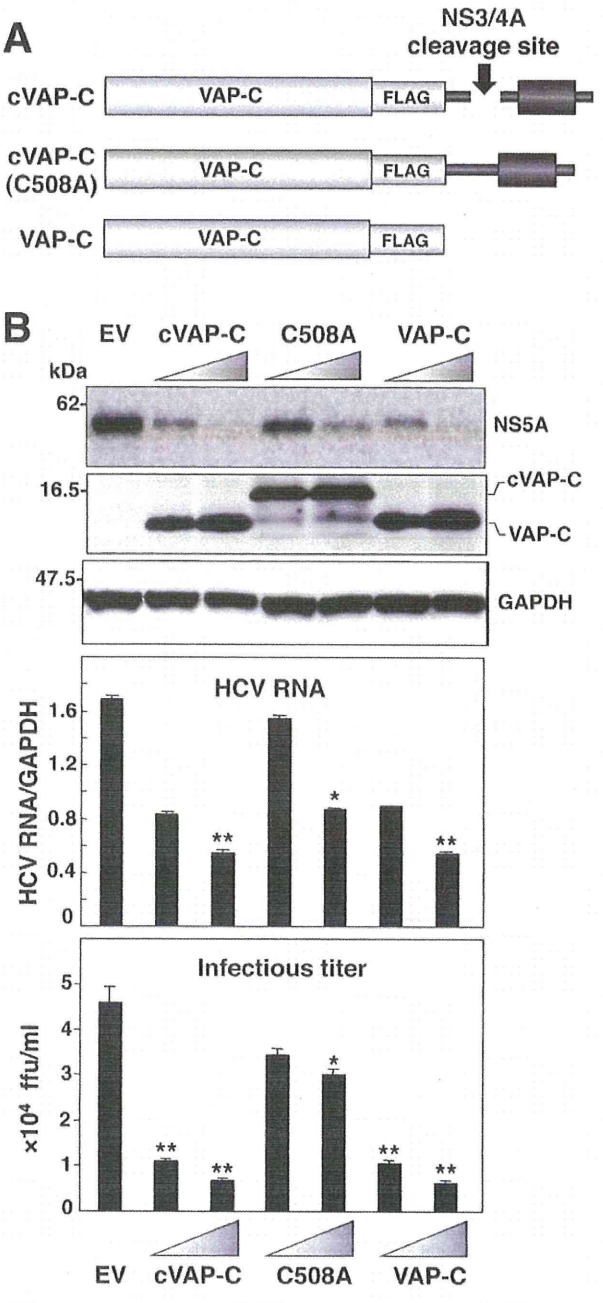

Figure 7. Suppression of HCV replication by the expression of cVAP-C. (A) Schematic representation of cVAP-C, cVAP-C(C508A) and VAP-C. Like cIRF7, cVAP-C is composed of the sequences of VAP-C, FLAG-tag, and the C-terminus domain of IPS-1. (B) Huh7OK1 cells (1.5×10^5 cells/well) infected with HCVcc at an moi of 1 and incubated for 72 h were transfected with EV, or plasmid encoding either cIRF7 or cIRF7(C508A), and the expressions of NS5A, VAP-Cs and GAPDH (top panel), synthesis of viral RNA (middle panel) and infectious titers in the culture supernatants were determined at 72 h post-transfection by immunoblotting, real-time PCR, and focus forming assay, respectively. The data shown in this figure are representative of three independent experiments. The error bars represent the standard deviations. Asterisks indicate significant differences (*$P<0.05$, **$P<0.01$) versus the control cells or mock-infected cells.
doi:10.1371/journal.pone.0015967.g007

encoding a GBV-B protease was amplified from pGBB (kindly provided by Dr. H. Akari) [41] by PCR and cloned into pcDNA3.1Flag/HA. The chimeric IRF7 (cIRF7) composed of the IRF7m fused with FLAG-tag and the C-terminus of human IPS-1 (from amino acid residues 503 to 540 amino acid residues) containing a cleavage site of HCV NS3/4A, transmembrane domain and the ER retention signal [21] (Fig. 2A) was cloned into pcDNA3.1-c-myc-His. A cIRF7 mutant, C508A, was generated to be resistant to HCV NS3/4A protease by substitution of Cys^{508} of cIRF7 to Ala. The reporter constructs of IFNα6, IFNβ, and ISRE were kindly provided by Drs. T. Kawai and S. Akira. All PCR products were confirmed by sequencing by an ABI PRISM 310 genetic analyzer (Applied Biosystems, Tokyo, Japan). The HCV NS3/4A protease inhibitor, BILN2061 was purchased from Acme Bioscience (Belmont, CA). Human recombinant IFNα and cyclosporine A (CsA) were purchased from PBL Biomedical Laboratories (New Brunswick, NJ) and Wako Pure Chemical Industries (Osaka, Japan), respectively.

Reporter assay

Huh7 cells, HCV replicon cells, and Huh7OK1 cells infected with HCVcc were seeded onto 12-well plates at the concentration of 1.5×10^5 cells/well and transfected with 100 ng of each of the plasmids encoding the luciferase gene under the control of the IFNα6, IFNβ and ISRE promoter together with the various constructs by using FuGene™6 (Roche Molecular Biochemicals, Mannheim, Germany). Luciferase activity was determined by the Dual-luciferase reporter assay system (Promega Inc., Madison, WI) and the *Renilla* luciferase reporter gene was simultaneously transfected as an internal control.

Immunoblotting

HCV replicon cells and Huh7OK1 cells infected with HCVcc were transfected with the plasmids encoding each of the wild-type and the dominant active mutants of IRFs and harvested at 72 h post-transfection. Cells were washed three times with ice-cold phosphate-buffered saline (PBS), suspended in lysis buffer containing 20 mM Tris-HCl (pH 7.4), 135 mM NaCl, 1% Triton X-100, 10% glycerol and protease inhibitor cocktail tablets (Roche Molecular Biochemicals) and centrifuged at 14,000×g for 15 min at 4°C after incubation for 30 min at 4°C. Cell lysates were subjected to sodium dodecyl sulfate-12.5% polyacrylamide gel electrophoresis (SDS-PAGE) after boiling in sample buffer and transferred to polyvinylidene difluoride membranes (Millipore, Tokyo, Japan). The membranes were blocked with PBS containing 0.05% Tween 20 and 5% skim milk at room temperature for 1 h, incubated with mouse monoclonal anti-FLAG M2 (Sigma), anti-hemagglutinin (HA) 16B12 (HA.11; BabCO, Richmond, CA), anti-NS5A mouse monoclonal antibody (Austral Biologicals, San Ramon, CA), anti-GAPDH (Santa Cruz Biotechnology, Santa Cruz, CA), or anti-hexahistidine monoclonal antibody (Santa Cruz) at room temperature for 1 h, and then with horseradish peroxidase-conjugated anti-mouse IgG or anti-rabbit IgG antibody at room temperature for 1 h. The immune complexes were visualized with Super Signal West Femto substrate (Pierce, Rockford, IL) and detected by an LAS-3000 image analyzer system (Fujifilm, Tokyo, Japan).

Quantitative reverse-transcription polymerase chain reaction (qRT-PCR)

A total RNA was prepared from HCV replicon cells and Huh7OK1 cells infected with HCVcc transfected with the plasmids encoding each of the IRF constructs using an RNeasy

mini kit (QIAGEN, Valencia, CA) and first-strand cDNA was synthesized by using ReverTra Ace (TOYOBO, Osaka, Japan) and oligo $(dT)_{20}$ primer. The expression of each cDNA was estimated by Platinum SYBR Green qPCR SuperMix UDG (Invitrogen) according to the manufacturer's protocol. Fluorescent signals were analyzed by an ABI PRISM 7000 (Applied Biosystems). The HCV and GAPDH genes were amplified using the primer pairs of 5′-GAGTGTCGTGCAGCCTCCA-3′ and 5′-CACTCGCAAGCACCCTATCA-3′, and 5′-ACCACAGTC-CATGCCATCAC-3′ and 5′-TCCACCACCCTGTTGCTGTA-3′, respectively. The expression of each of mRNA was normalized with that of GAPDH.

Subcellular localization of cIRF7 in HCV- replicating cells

Cells transfected with the plasmids were harvested at 24 h post transfection, washed twice with PBS, fixed with PBS containing 4% paraformaldehyde, and permeabilized by incubation with PBS containing 0.25% saponin for 10 min. Cells were incubated for 1 h at 4°C with 1μg/ml of anti-NS3 (251) mouse monoclonal antibody (Santa Cruz), anti-NS5A mouse monoclonal antibody (Austral Biologicals), or mouse monoclonal antibody to protein disulfide isomerase (PDI) (Affinity Bioreagents, Golden, CO) in PBS containing 10% FCS (PBSF), and then incubated at room temperature for 1 h with 0.5 μg/ml of Alexa Flour 594-conjugated anti-mouse IgG (Molecular Probes, Eugene, OR) after three time washes with PBSF. Cell nuclei were stained with 4′, 6-diamidino-2-phenylindole (DAPI). After an extensive wash with PBSF, the samples were examined with a Fluoview FV1000 laser scanning confocal microscope (OLYMPUS, Tokyo, Japan).

Statistical analysis. Results were expressed as the mean ± standard deviation. The significance of differences in the means was determined by Student's *t* test.

Acknowledgments

The authors gratefully thank H. Murase for her secretarial work. We also thank R. Bartenschlager, T. Wakita, H. Akari, T. Kawai and S. Akira for providing cell lines and plasmids.

Author Contributions

Conceived and designed the experiments: TA Y. Matsuura. Performed the experiments: XW TA HK ST Y. Mori HT KM. Analyzed the data: NK TS MT. Contributed reagents/materials/analysis tools: NK MT. Wrote the paper: TA Y. Matsuura.

References

1. Cerny A, Chisari FV (1999) Pathogenesis of chronic hepatitis C: immunological features of hepatic injury and viral persistence. Hepatology 30: 595–601.
2. Moriishi K, Matsuura Y (2003) Mechanisms of hepatitis C virus infection. Antivir Chem Chemother 14: 285–297.
3. Fried MW (2002) Side effects of therapy of hepatitis C and their management. Hepatology 36: S237–244.
4. Wakita T, Pietschmann T, Kato T, Date T, Miyamoto M, et al. (2005) Production of infectious hepatitis C virus in tissue culture from a cloned viral genome. Nat Med 11: 791–796.
5. Sen GC (2001) Viruses and interferons. Annu Rev Microbiol 55: 255–281.
6. Darnell JE, Jr., Kerr IM, Stark GR (1994) Jak-STAT pathways and transcriptional activation in response to IFNs and other extracellular signaling proteins. Science 264: 1415–1421.
7. Heim MH, Moradpour D, Blum HE (1999) Expression of hepatitis C virus proteins inhibits signal transduction through the Jak-STAT pathway. J Virol 73: 8469–8475.
8. Blindenbacher A, Duong FH, Hunziker L, Stutvoet ST, Wang X, et al. (2003) Expression of hepatitis C virus proteins inhibits interferon alpha signaling in the liver of transgenic mice. Gastroenterology 124: 1465–1475.
9. Zhu H, Nelson DR, Crawford JM, Liu C (2005) Defective Jak-Stat activation in hepatoma cells is associated with hepatitis C viral IFN-alpha resistance. J Interferon Cytokine Res 25: 528–539.
10. Yoneyama M, Kikuchi M, Natsukawa T, Shinobu N, Imaizumi T, et al. (2004) The RNA helicase RIG-I has an essential function in double-stranded RNA-induced innate antiviral responses. Nat Immunol 5: 730–737.
11. Yoneyama M, Kikuchi M, Matsumoto K, Imaizumi T, Miyagishi M, et al. (2005) Shared and unique functions of the DExD/H-box helicases RIG-I, MDA5, and LGP2 in antiviral innate immunity. J Immunol 175: 2851–2858.
12. Kawai T, Akira S (2006) Innate immune recognition of viral infection. Nat Immunol 7: 131–137.
13. Honda K, Takaoka A, Taniguchi T (2006) Type I interferon [corrected] gene induction by the interferon regulatory factor family of transcription factors. Immunity 25: 349–360.
14. Li K, Foy E, Ferreon JC, Nakamura M, Ferreon AC, et al. (2005) Immune evasion by hepatitis C virus NS3/4A protease-mediated cleavage of the Toll-like receptor 3 adaptor protein TRIF. Proc Natl Acad Sci USA 102: 2992–2997.
15. Meylan E, Curran J, Hofmann K, Moradpour D, Binder M, et al. (2005) Cardif is an adaptor protein in the RIG-I antiviral pathway and is targeted by hepatitis C virus. Nature 437: 1167–1172.
16. Li XD, Sun L, Seth RB, Pineda G, Chen ZJ (2005) Hepatitis C virus protease NS3/4A cleaves mitochondrial antiviral signaling protein off the mitochondria to evade innate immunity. Proc Natl Acad Sci USA 102: 17717–17722.
17. Loo YM, Owen DM, Li K, Erickson AK, Johnson CL, et al. (2006) Viral and therapeutic control of IFN-β promoter stimulator 1 during hepatitis C virus infection. Proc Natl Acad Sci USA 103: 6001–6006.
18. Lin R, Lacoste J, Nakhaei P, Sun Q, Yang L, et al. (2006) Dissociation of a MAVS/IPS-1/VISA/Cardif-IKKepsilon molecular complex from the mitochondrial outer membrane by hepatitis C virus NS3-4A proteolytic cleavage. J Virol 80: 6072–6083.
19. Vilasco M, Larrea E, Vitour D, Dabo S, Breiman A, et al. (2006) The protein kinase IKKepsilon can inhibit HCV expression independently of IFN and its own expression is downregulated in HCV-infected livers. Hepatology 44: 1635–1647.
20. Kukihara H, Moriishi K, Taguwa S, Tani H, Abe T, et al. (2009) Human VAP-C negatively regulates hepatitis C virus propagation. J Virol 83: 7959–7969.
21. Tanaka Y, Mori Y, Tani H, Abe T, Moriishi K, et al. (2010) Establishment of an indicator cell system for hepatitis C virus. Microbiology and immunology 54: 206–220.
22. Lin R, Heylbroeck C, Pitha PM, Hiscott J (1998) Virus-dependent phosphorylation of the IRF-3 transcription factor regulates nuclear translocation, transactivation potential, and proteasome-mediated degradation. Mol Cell Biol 18: 2986–2996.
23. Lin R, Genin P, Mamane Y, Hiscott J (2000) Selective DNA binding and association with the CREB binding protein coactivator contribute to differential activation of alpha/beta interferon genes by interferon regulatory factors 3 and 7. Mol Cell Biol 20: 6342–6353.
24. Lin R, Mamane Y, Hiscott J (2000) Multiple regulatory domains control IRF-7 activity in response to virus infection. J Biol Chem 275: 34320–34327.
25. Ning S, Hahn AM, Huye LE, Pagano JS (2003) Interferon regulatory factor 7 regulates expression of Epstein-Barr virus latent membrane protein 1: a regulatory circuit. J Virol 77: 9359–9368.
26. Chen Z, Benureau Y, Rijnbrand R, Yi J, Wang T, et al. (2007) GB virus B disrupts RIG-I signaling by NS3/4A-mediated cleavage of the adaptor protein MAVS. J Virol 81: 964–976.
27. Namba K, Naka K, Dansako H, Nozaki A, Ikeda M, et al. (2004) Establishment of hepatitis C virus replicon cell lines possessing interferon-resistant phenotype. Biochem Biophys Res Commun 323: 299–309.
28. Naka K, Takemoto K, Abe K, Dansako H, Ikeda M, et al. (2005) Interferon resistance of hepatitis C virus replicon-harbouring cells is caused by functional disruption of type I interferon receptors. J Gen Virol 86: 2787–2792.
29. Lev S, Halevy DBen, Peretti D, Dahan N (2008) The VAP protein family: from cellular functions to motor neuron disease. Trends in cell biology 18: 282–290.
30. Soriano V, Madejon A, Vispo E, Labarga P, Garcia-Samaniego J, et al. (2008) Emerging drugs for hepatitis C. Expert Opin Emerg Drugs 13: 1–19.
31. Zeuzem S (2008) Interferon-based therapy for chronic hepatitis C: current and future perspectives. Nat Clin Pract Gastroenterol Hepatol 5: 610–622.
32. Vignuzzi M, Stone JK, Arnold JJ, Cameron CE, Andino R (2006) Quasispecies diversity determines pathogenesis through cooperative interactions in a viral population. Nature 439: 344–348.
33. Abe T, Kaname Y, Hamamoto I, Tsuda Y, Wen X, et al. (2007) Hepatitis C virus nonstructural protein 5A modulates the toll-like receptor-MyD88-dependent signaling pathway in macrophage cell lines. J Virol 81: 8953–8966.
34. Zhang T, Lin RT, Li Y, Douglas SD, Maxcey C, et al. (2005) Hepatitis C virus inhibits intracellular interferon alpha expression in human hepatic cell lines. Hepatology 42: 819–827.
35. Chen L, Borozan I, Feld J, Sun J, Tannis LL, et al. (2005) Hepatic gene expression discriminates responders and nonresponders in treatment of chronic hepatitis C viral infection. Gastroenterology 128: 1437–1444.
36. Sarasin-Filipowicz M, Oakeley EJ, Duong FH, Christen V, Terracciano L, et al. (2008) Interferon signaling and treatment outcome in chronic hepatitis C. Proc Natl Acad Sci USA 105: 7034–7039.

37. Cheng G, Zhong J, Chisari FV (2006) Inhibition of dsRNA-induced signaling in hepatitis C virus-infected cells by NS3 protease-dependent and -independent mechanisms. Proc Natl Acad Sci USA 103: 8499–8504.
38. Okamoto T, Omori H, Kaname Y, Abe T, Nishimura Y, et al. (2008) A single-amino-acid mutation in hepatitis C virus NS5A disrupting FKBP8 interaction impairs viral replication. J Virol 82: 3480–3489.
39. Lohmann V, Korner F, Koch J, Herian U, Theilmann L, et al. (1999) Replication of subgenomic hepatitis C virus RNAs in a hepatoma cell line. Science 285: 110–113.
40. Okamoto K, Moriishi K, Miyamura T, Matsuura Y (2004) Intramembrane proteolysis and endoplasmic reticulum retention of hepatitis C virus core protein. J Virol 78: 6370–6380.
41. Bukh J, Apgar CL, Yanagi M (1999) Toward a surrogate model for hepatitis C virus: An infectious molecular clone of the GB virus-B hepatitis agent. Virology 262: 470–478.

ELSEVIER

INSTITUT PASTEUR

Microbes and Infection 13 (2011) 405–412

www.elsevier.com/locate/micinf

Original article

Intracellular delivery of serum-derived hepatitis C virus

Takasuke Fukuhara [a,b], Hideki Tani [a], Mai Shiokawa [a], Yukinori Goto [a], Takayuki Abe [a], Akinobu Taketomi [b], Ken Shirabe [b], Yoshihiko Maehara [b], Yoshiharu Matsuura [a,*]

[a] *Department of Molecular Virology, Research Institute for Microbial Diseases, Osaka University, 3-1 Yamada-oka, Suita, Osaka 565-0871, Japan*
[b] *Department of Surgery and Science, Graduate School of Medical Sciences, Kyushu University, Fukuoka, Japan*

Received 7 September 2010; accepted 11 January 2011
Available online 22 January 2011

Abstract

A robust and reliable cell culture system for serum-derived HCV (HCVser) has not been established yet because of the presence of neutralizing antibody and tropism for infection. To overcome this obstacle, we employed a lipid-mediated protein intracellular delivery reagent (PIDR) that permits internalization of proteins into cells. Although entry of HCVcc was not enhanced by the treatment with PIDR, entry of HCVser into hepatoma cell lines (Huh7 and HepG2) and immortalized primary hepatocytes (Hc and HuS/E2) was significantly enhanced by the PIDR treatment. The entry of HCVser into Huh7 cells in the presence of PIDR was resistant to the neutralization by an anti-hCD81 antibody, suggesting that PIDR is capable of internalizing HCVser in a receptor-independent manner. Interestingly, the PIDR-mediated entry of HCVser and HCVcc was enhanced by the addition of sera from chronic hepatitis C patients but not from healthy donors. In addition, neutralization of HCVcc infection by anti-E2 antibody was canceled by the treatment with PIDR. In conclusion, the PIDR is a valuable tool to get over the obstacle of neutralizing antibodies to internalize HCV into cells and might be useful for the establishment of *in vitro* propagation HCVser.

Keywords: Hepatitis C virus; Protein intracellular delivery; Serum-derived virus

1. Introduction

More than 170 million individuals worldwide are infected with hepatitis C virus (HCV), and hepatic steatosis, cirrhosis and hepatocellular carcinoma (HCC) induced by HCV infection are life-threatening [1]. Although combined-therapy with peg-interferon (IFN) and ribavirin has achieved a sustained virological response in 50% of individuals infected with HCV genotype 1 [2], a more effective therapeutic modality for HCV infection is needed [3]. To this end, further detailed analyses of HCV are needed in order to clarify not only the viral life cycle but also the pathogenesis. Although cell culture systems for HCV (HCVcc) have been established based on the JFH-1 strain isolated from a fulminant hepatitis C patient [4], such systems were unable to establish chronic infection in chimpanzees [4] or to induce cell damage and inflammation in chimeric mice xenotransplanted with human hepatocytes [5], and therefore establishment of a robust cell culture system capable of propagating serum-derived HCV (HCVser) from hepatitis C patients is required.

Although previous reports suggested a partial replication of HCVser in the primary hepatocytes (PHH) freshly isolated from human liver [6], the level of viral RNA replication was low and reconfirmation of the viral propagation was not achieved due to the difficulty of providing a stable supply of the PHH. Recently, it was shown that a three-dimensional culture system of immortalized PHH was capable of propagating the HCVser from chronic hepatitis C patients [7,8]. HCVser in the patients was slightly amplified in these culture systems, but the levels of viral RNA replication were far lower than those of HCVcc in Huh7-derived adaptive cell lines. Part of the difficulty in establishing a cell culture system for HCVser might be attributable to: i) the

Abbreviations: HCV, hepatitis C virus; IFN, interferon; PHH, primary human hepatocyte; PIDR, protein intracellular delivery reagent; PCR, polymerase chain reaction; VSV, vesicular stomatitis virus.

* Corresponding author. Fax: +81 6 6879 8269.
E-mail address: matsuura@biken.osaka-u.ac.jp (Y. Matsuura).

1286-4579/$ - see front matter © 2011 Institut Pasteur. Published by Elsevier Masson SAS. All rights reserved.
doi:10.1016/j.micinf.2011.01.005

existence of high titers of neutralizing antibodies in the sera of hepatitis C patients [9]; ii) the heterogeneity of HCV particles (quasispecies), which exhibit different cell tropisms for infection and replication [10]; and iii) the inconsistent expression of the putative receptors for HCV entry, including CD81, SR-BI, claudin-1 and occludin [11]. It may be necessary to overcome these obstacles before a robust and reliable *in vitro* cell culture system can be established for HCVser.

Polybrene has been used for the efficient infection of retrovirus [12], and spinoculation has also been employed to accelerate the entry of various viruses, including retrovirus [13] and murine coronavirus [14]. Entry of HCVcc into not only the permissive cell line Huh7.5.1 but also the non-permissive cell line PLC/PRF/5 has been shown to be enhanced by spinoculation [15,16]. In this study, we examined the effects of these accelerating procedures for entry of HCVser and found that a cationic amphiphilic-based lipid-mediated protein intracellular delivery reagent (PIDR) [17] exhibited a potent enhancement of entry of HCVser. Our data suggest that PIDR allows complex formation with viral particles via both electrostatic and hydrophobic interactions and enhances internalization of the HCVser into cells in a receptor-independent manner.

2. Materials and methods

2.1. Sera

Sera from chronic hepatitis C patients and a cured patient possessing the anti-HCV antibodies were obtained at the Kyushu University Hospital after obtaining full informed consent from all patients. Seven serum samples from hepatitis C patients, including two window-period serum samples without any detectable anti-HCV antibodies, were obtained from the Benesis Corporation (Osaka, Japan). Human sera from healthy donors were obtained from Sigma–Aldrich Inc. (St. Louis, MO). Sera from healthy donors, chronic hepatitis patients and acute hepatitis patients were designated HDS, CHS, and AHS, respectively. The HCV-RNA titers of CHS and AHS were 7.15 ± 0.34 (range: 6.6–7.5) and 8.20 ± 0.14 (range: 8.1–8.3), respectively. The genotypes of HCV in these sera were 1a (7 patients) and 1b (11 patients).

2.2. Human liver cell lines and preparation of HCVcc

HepG2 and HEK-293T cell lines were obtained from the American Type Culture Collection (Rockville, MD). The Huh7OK1 cell line exhibits an efficient propagation of HCVcc as described previously [18]. The HepCD81 cell line stably expressing human CD81 was established as described previously [19]. HuS-E/2 was kindly provided by M. Hijikata, Kyoto University [20]. Hc (an immortalized human liver cell line) was purchased from the Applied Cell Biology Research Institute (Kirkland, WA). These cell lines were cultured in Dulbecco's modified Eagle's medium (DMEM) (Sigma) containing 10% fetal bovine serum (FBS). The *in vitro* transcribed RNA of the JFH-1 strain of HCV was introduced into Huh7OK1 cells [21] and culture supernatants were collected at 7 days post-transfection and used as HCVcc. The infectivity of HCVcc was determined by focus forming assay as previously described [19].

2.3. Transfection of plasmids and intracellular delivery of proteins

The plasmids were transfected into cells by liposome-mediated transfection using *Trans*IT-LT1 (Mirus, Madison, WI). The proteins were introduced into cells by PIDR (PULSin; Polyplus-transfection Inc., New York, NY) according to the manufacturer's protocol. FITC-conjugated mouse IgG antibody (Invitrogen Molecular Probes, Eugene, OR) or recombinant phycoerythrin (PE; Polyplus-transfection Inc.) was introduced into cells by the PIDR as a positive control.

2.4. Quantitative reverse-transcription polymerase chain reaction (qRT-PCR)

Total RNA was prepared from cells using an RNeasy mini kit (Qiagen, Tokyo, Japan). The synthesis of first-strand cDNA and qRT-PCR was performed using TaqMan EZ RT-PCR Core Reagents and ABI Prism 7000 system (Applied Biosystems Japan, Tokyo, Japan) according to the manufacturer's protocol. The primers for Taqman PCR were designed in a non-coding region as previously reported [22].

2.5. Infection of HCVser and HCVcc by spinoculation, polybrene and PIDR

Cells were seeded at 1×10^5 cells/well in a 48-well plate and cultured for 24 h. For spinoculation, 2 μl of HCV-positive serum or HCVcc at a multiplicity of infection (MOI) of 0.05 were inoculated into cells and immediately centrifuged at 500× *g* for 120 min at room temperature. For infection of HCV by polybrene and PIDR, 2 μg of polybrene or 1.5 μl of PIDR were incubated with HCV-positive serum or HCVcc diluted in 20 μl of phosphate-buffered saline (PBS) for 15 min at room temperature to allow complex formation [12]. Cells were trypsinized at 24 h post-inoculation, seeded in a 48-well plate to remove non-specific binding of HCV, and cultured for several days.

2.6. Production and infection of pseudotype vesicular stomatitis virus (VSV)

Pseudotype VSVs were generated as described previously [19]. The pseudotype VSVs, VSVpv/GFP and VSVpv/luc, bore the VSVG protein on the virion surface and replaced the G envelope gene with the green fluorescent protein (GFP) and luciferase genes, respectively. Pseudotype VSV bearing HCV E1 and E2 glycoproteins (HCVpv) was prepared as described previously [19]. These pseudotype viruses were inoculated into Huh7OK1 cells in the presence or absence of PIDR together with or without anti-VSVG polyclonal antibody (ab34774; Abcam Inc., Cambridge, MA) or CHS, and infectivity was determined at 24 h post-infection by the expression of GFP or luciferase activity after treatment with a passive lysis buffer (Promega Co., Madison, WI).

2.7. Inhibition of HCVcc and HCVser infection by the treatment with antibody against human CD81 and anti-E2 antibody (AP-33)

To determine the involvement of human CD81 in the intracellular delivery of HCV by PIDR, Huh7OK1 cells were pre-treated with 5 μg/ml of anti-human CD81 monoclonal antibody (JS-81; BD Biosciences Pharmingen, Mountain View, CA) for 1 h at 37 °C and then inoculated with HCVcc or HCVser in the presence of PIDR. Anti-E2 monoclonal antibody (AP-33) was kindly provided by A.H. Patel, University of Glasgow [23]. AP-33 was pre-mixed with HCVcc for 1 h with or without PIDR and then cells were incubated with this mixture and cultured for several days.

3. Results

3.1. Effect of spinoculation and polybrene on the entry of HCVser and HCVcc

First, we examined the effect of spinoculation on the entry of HCVser or HCVcc. Intracellular HCV-RNA titers of Huh7OK1 cells upon infection of HCVser and HCVcc with or without spinoculation at 24 h post-infection were determined (Data not shown). Although entry of HCVcc into Huh7OK1 cells was 10-fold increased by the spinoculation, no effect was observed in the entry of HCVser. Next, we examined the effect of polybrene on the entry of HCVser and HCVcc into Huh7OK1 cells. Although polybrene induced a slight increase of the entry of HCVcc, no significant effect on the entry of HCVser was observed intracellularly at 24 h post-infection (Data not shown). These results indicated that neither spinoculation nor polybrene induced an enhancement of the entry of HCVser.

3.2. Internalization of viral particles by PIDR

To determine the efficacy of intracellular delivery of proteins by PIDR, FITC-conjugated mouse IgG and recombinant PE were introduced into Huh7OK1 cells by PIDR. Both FITC-conjugated IgG and PE were efficiently internalized into Huh7OK1 cells by the treatment with PIDR but not by the lipofection (Fig. 1A). Next, to determine the receptor-independent entry of viral particles into cells by the PIDR, the expression of GFP upon infection of a pseudotype VSV lacking VSVG (VSVΔGpv/GFP) into Huh7OK1 cells was examined. Although VSVΔGpv/GFP lost infectivity due to a lack of the G glycoprotein, the addition of PIDR facilitated entry of the particles (Fig. 1A). To further examine the effect of the presence of neutralization antibody on the delivery of viral particles by PIDR, the expression of GFP upon transduction of VSVpv/GFP into Huh7OK1 cells in the presence of neutralization antibody and PIDR was examined. Although VSVpv/GFP exhibited a high infectivity to Huh7OK1 cells and the infection was completely neutralized by the anti-VSVG antibody, treatment with PIDR partially recovered the infectivity of VSVpv/GFP neutralized by the antibody (Fig. 1B). Similar results were confirmed by using VSVΔGpv/luc and VSVpv/luc carrying the luciferase gene as a reporter (Fig. 1C). These results indicate that PIDR is a useful tool to facilitate the entry of viral particles into target cells, irrespective of the authenticity of the envelope proteins of the particles or the presence of the neutralizing antibodies.

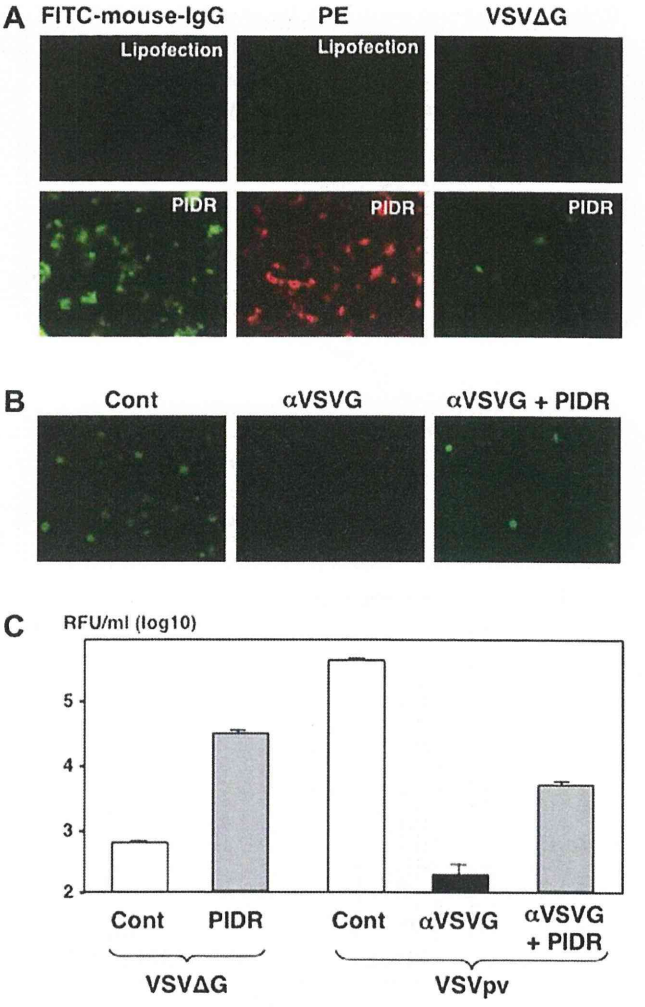

Fig. 1. Characterization of the intracellular delivery of proteins and viral particles by PIDR. (A) FITC-conjugated mouse IgG (left panels) or recombinant PE (center panels) was introduced into Huh7OK1 cells by the treatment with PIDR or a lipofection reagent. The expression of GFP upon infection of a pseudotype VSV lacking VSVG (VSVΔGpv/GFP) into Huh7OK1 cells in the presence (lower panel) and absence (upper panel) of PIDR was examined (right panels). (B) The effect of the presence of neutralization antibody on the delivery of viral particles by PIDR. Expression of GFP upon transduction of a VSVpv/GFP into Huh7OK1 cells in the presence of neutralization antibody and PIDR was examined. (C) The receptor-independent entry of viral particles was confirmed by using VSVΔGpv/luc and VSVpv/luc carrying the luciferase gene as a reporter.

3.3. Effect of PIDR on the infection with HCVcc

To determine the effect of PIDR on the infection of HCV, HCVcc was inoculated into Huh7OK1 cells at an MOI of 0.05 in the presence or absence of PIDR and intracellular viral

RNA was measured every 24 h. No significant difference in the infection of HCVcc was observed by the addition of PIDR (Fig. 2A). Next, to mimic the infection of HCV in the presence of neutralization antibodies, HCVcc was mixed with CHS and inoculated into Huh7OK1 cells. Although infection of HCVcc into Huh7OK1 was completely neutralized by the incubation with CHS, addition of PIDR recovered the infectivity of HCVcc (Fig. 2B). Furthermore, to confirm the effect of PIDR on the internalization of HCVcc interacting with neutralizing antibody, HCVcc was pre-incubated with AP-33 and inoculated into Huh7OK1 cells. Although infection of HCVcc was neutralized by the treatment with AP-33 in a dose-dependent manner, the neutralization by AP-33 was canceled by the treatment with PIDR (Fig. 2C). These results suggest that PIDR has the ability to internalize HCVcc even in the presence of neutralizing antibodies.

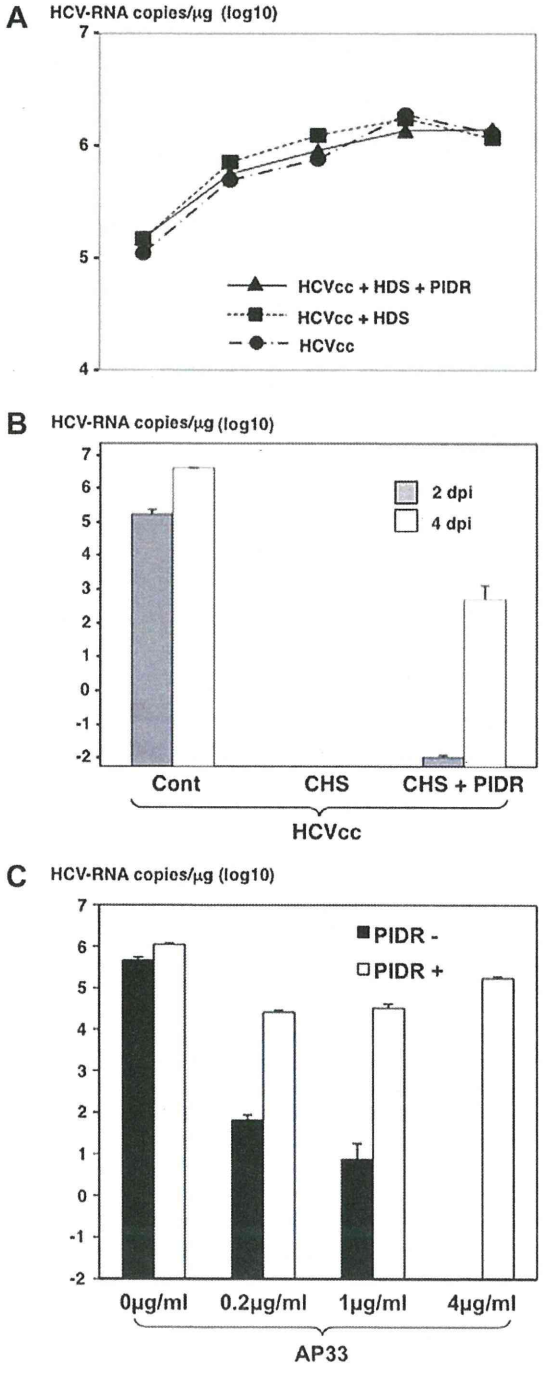

Fig. 2. Effect of PIDR on the infection with HCVcc. (A) HCVcc was inoculated into Huh7OK1 cells at an MOI of 0.05 in the presence or absence of healthy donor sera (HDS) and PIDR and intracellular viral RNA was measured every 24 h (B) HCVcc was mixed with sera from chronic hepatitis C patients (CHS) or/and PIDR and inoculated into Huh7OK1 cells. (C) HCVcc was premixed with anti-E2 monoclonal antibody (AP-33) and inoculated into Huh7OK1 cells in the presence or absence of PIDR.

3.4. Effect of PIDR on the infection of HCVser

The efficient neutralizing activities of HCV infection in CHS were comfirmed by a neutralization assay using pseudotype viruses. Infection of HCVpv bearing HCV E1 and E2 proteins but not of VSVpv bearing VSVG protein was significantly neutralized by the CHS (Fig. 3A). Next, to determine the effect of PIDR on the entry of HCVser in the presence of neutralizing antibodies, HCVser and CHS possessing the neutralizing antibodies against HCV were inoculated into Huh7OK1 cells with or without incubation with PIDR. Huh7OK1 cells inoculated with CHS pre-incubated with PIDR exhibited significantly higher HCV-RNA titers at 24 h post-infection than those without the treatment (Fig. 3B). Furthermore, to determine the amount of HCV internalized into cells, Huh7OK1 cells inoculated with CHS treated with PIDR were trypsinized and reseeded into a new culture plate at 24 h post-infection. HCV-RNA was detected in cells inoculated CHS pre-incubated with PIDR but not in those without PIDR treatment at 24 h after reseeding (Fig. 3C). These results indicate that treatment with PIDR permits HCVser to internalize into target cells even in the presence of neutralizing antibodies.

3.5. Neutralizing antibodies in sera from chronic hepatitis C patients enhance PIDR-mediated entry of HCV

No reduction of infectivity of HCVpv and VSVpv was observed by the incubation with AHS, suggesting that AHS possesses no detectable neutralizing antibodies to HCV (Fig. 4A). To examine the effect of neutralizing antibody on the intracellular delivery of HCVser by PIDR, AHS was incubated with the CHS carrying neutralization antibodies but no infectious HCV obtained from patients cured by the interferon therapy in the presence or absence of PIDR and inoculated into Huh7OK1 cells. Internalization of HCV in AHS was increased two-fold by the treatment with PIDR. However, intracellular viral RNA titer was slightly decreased by the incubation with CHS in the absence of PIDR, probably due to the neutralization by the antibodies, and addition of PIDR resulted in a three-fold enhancement of the entry of HCV in AHS in the presence of CHS compared with that in the absence of CHS (Fig. 4B). Next, Huh7OK1 cells were inoculated with HCVcc at an MOI of 0.05 after incubation with 0.4–40 μl/ml of HCV-negative CHS in the presence or absence of PIDR. Although infection of HCVcc was

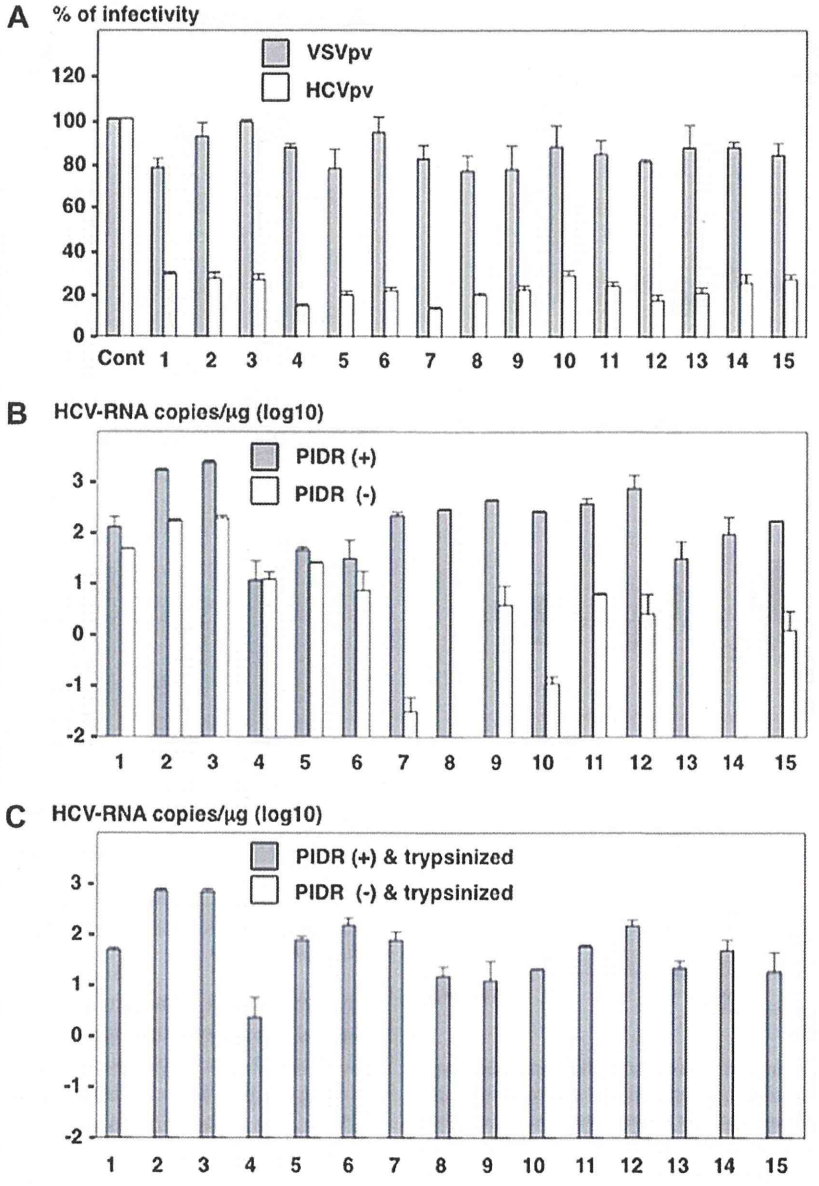

Fig. 3. Effect of PIDR on the infection with HCVser. (A) The neutralizing effect of antibodies in the CHS was determined by a neutralization assay using the pseudotype viruses. White and gray bars indicated VSVpv and HCVpv, respectively. (B) The effect of PIDR on the entry of HCVser in the CHS into Huh7OK1 cells. HCV-RNA titers in cells 24 h post-inoculation with HCVser in the presence and absence of PIDR are indicated by gray and white bars, respectively. (C) To determine the internalization of HCVser into Huh7OK1 cells, cells inoculated with the CHS in the presence (gray bar) or absence (white bars) of PIDR were trypsinized and reseeded into a new culture plate at 24 h post-infection, and HCV-RNA titers in the cells were determined at 24 h post-inoculation.

neutralized by CHS in a dose-dependent manner, addition of PIDR enhanced the infection of HCVcc in the presence of CHS in a dose-dependent manner (Fig. 4C). These results indicate that PIDR facilitates entry of HCVser in the presence of neutralizing antibody.

3.6. Human CD81-independent entry of HCVser by PIDR

Next, to determine the involvement of human CD81 (hCD81), a major receptor candidate for HCV [24], on the PIDR-mediated entry of HCVser, Huh7OK1 cells were pre-treated with anti-hCD81 antibody and inoculated with HCVser treated with PIDR. Although pretreatment with anti-hCD81 antibody resulted in a significant reduction in the entry of HCVser, treatment with PIDR enhanced the entry of HCVser irrespective of the presence of the anti-human CD81antibody (Fig. 5A). In addition, although entry of HCVser into HepG2 and HepCD81 cells was low and independent of the expression of hCD81, treatment with PIDR enhanced the entry of HCVser irrespective of the expression of human CD81 (Fig. 5B). These results suggest that the PIDR-mediated entry of HCVser is independent of the expression of hCD81 and is effective for the entry of HCVser into various cell lines other than Huh7-derived cell lines.

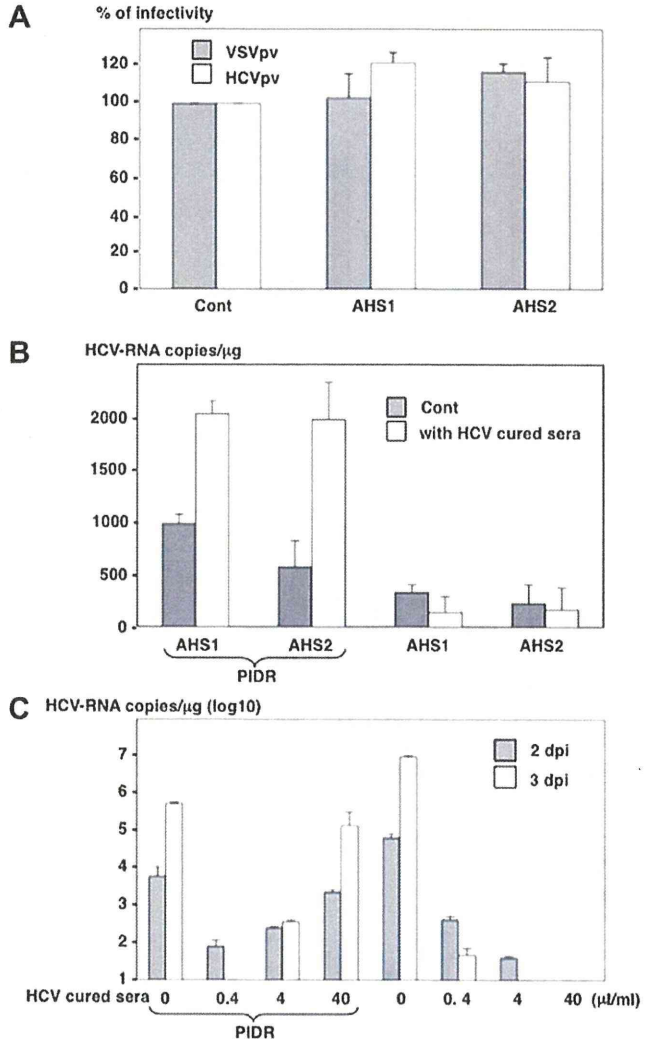

Fig. 4. Neutralizing antibodies in the CHS enhanced the PIDR-mediated entry of HCV. (A) The absence of neutralizing antibodies in the sera from acute hepatitis C patients (AHS) was determined by a neutralization assay using the HCVpv (white bars) and VSVpv (gray bar). (B) The effect of PIDR on the entry of HCVser into Huh7OK1 cells in the presence of neutralizing antibodies. The AHS were incubated with the CHS carrying neutralization antibodies but no infectious HCV obtained from patients cured by the IFN therapy (white bars) or HDS (gray bar) in the presence (left) or absence (right) of PIDR and inoculated into Huh7OK1 cells. The HCV-RNA titers in cells were determined at 24 h post-inoculation. (C). The effect of neutralizing antibodies on the PIDR-mediated infection of HCVcc. Huh7OK1 cells were inoculated with HCVcc at an MOI of 0.05 after incubation with 0.4–40 μl/ml of HCV-negative CHS in the presence (left) or absence (right) of PIDR. Gray and white bars indicate the HCV-RNA titers at 2 and 3 days after infection, respectively.

3.7. Effect of PIDR on the entry of HCVser into immortalized human hepatocytes

Recently, Aly et al. reported that immortalized human hepatocytes, HuS/E2 cells, exhibited a high susceptibility to the infection with HCVser [7]. Therefore, we examined the effect of PIDR on the entry of HCVser into immortalized human hepatocytes, including Hc and HuS/E2 cells. The addition of PIDR enhanced the entry of HCVser into both Hc and HuS/E2 cells

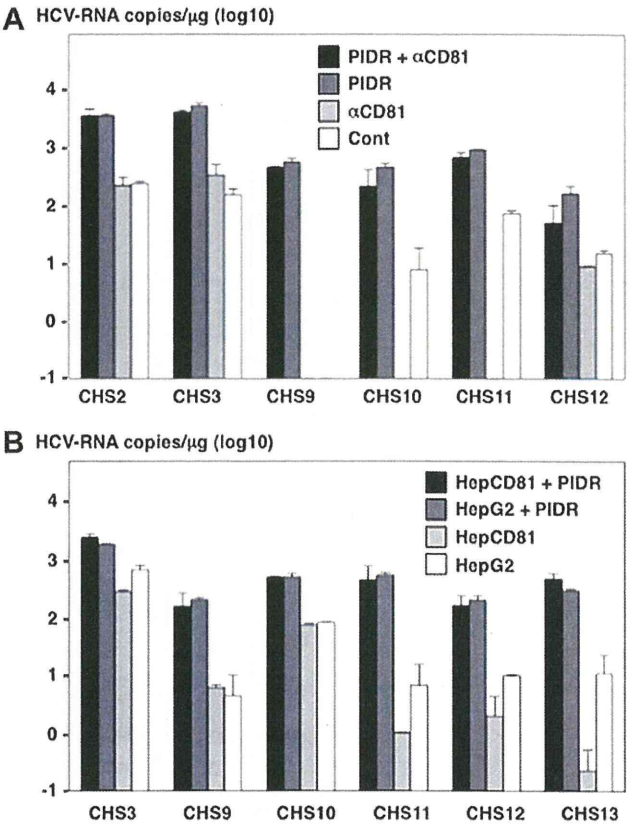

Fig. 5. Human CD81-independent entry of HCVser by PIDR. (A) The effect of anti-hCD81 antibody on the entry of HCVser into Huh7OK1 cells in the presence or absence of PIDR. (B) The effect of PIDR on the entry of HCVser into HepG2 and HepCD81 cells. HCV-RNA titers in cells were determined at 24 h post-inoculation.

(Fig. 6A and B). These results indicate that PIDR has the potential to enhance the entry of HCVser into not only cancer cell lines but also immortalized hepatocytes. Next, to evaluate the long-term effect of PIDR treatment on the infectivity of HCVser, Hc cells inoculated with CHS pre-incubated with PIDR were cultured for a long period. HCV-RNA could be detected at 10, 15 and 20 days after PIDR-mediated infection (Fig. 6C). However, significant elevations of HCV-RNA titers were not seen (Data not shown).

4. Discussion

In this study, we examined the efficiency of intracellular deliveries of HCVser by using spinoculation, polybrene and PIDR and found that the PIDR exhibited the highest efficacy on the entry of HCVser into target cells. Especially, trypsinization and reseeding of cells dramatically reduced HCV-RNA levels in groups that were not treated with PIDR as compared to those were treated with PIDR (Fig. 3B and C), and PIDR treatment dramatically increased the internalization of HCVcc treated with CHS or AP-33 at 2 and 4 days after infection (Fig. 2B and C). These results suggest that PIDR is feasible to deliver HCV/CHS complexes into target cells that allow productive infection. In addition, PIDR facilitated the entry of

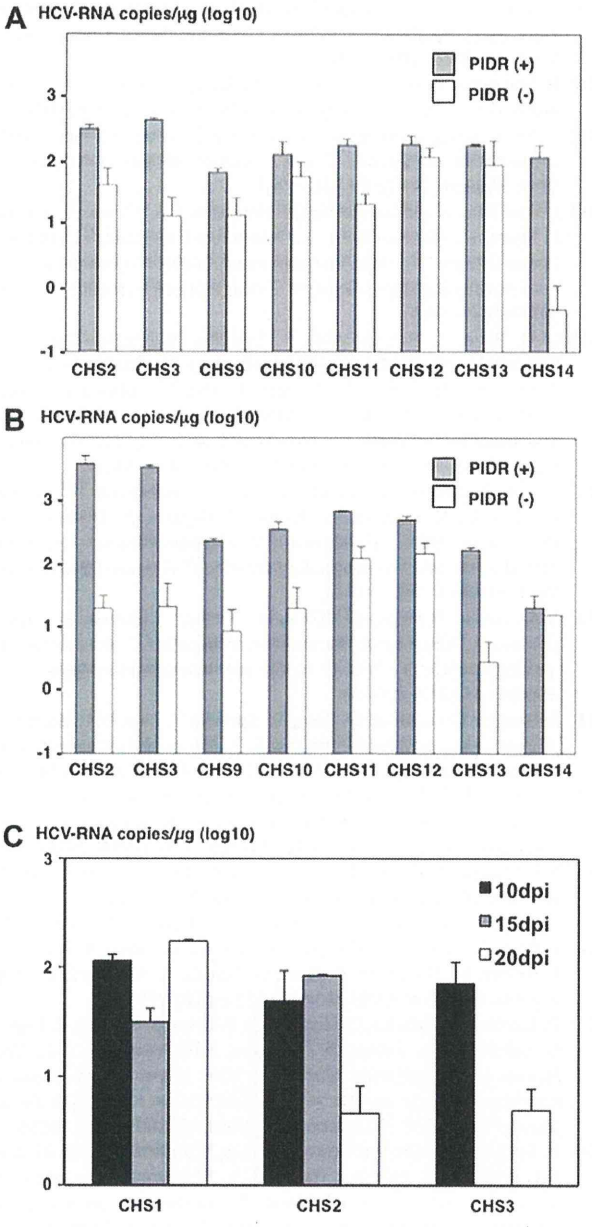

Fig. 6. Effect of PIDR on the entry of HCVser into immortalized human hepatocytes. The effect of PIDR on the entry of HCVser into immortalized human hepatocytes, such as Hc (A) and HuS/E2 (B) cells. The HCV-RNA titers in cells were determined at 24 h post-inoculation. (C) HCV-RNA titers in Hc cells inoculated with HCVser were evaluated at 10, 15 and 20 days after PIDR-mediated infection.

HCVser into the hepatoma cell lines and immortalized human hepatocytes in an hCD81-independent manner. Furthermore, we demonstrated that the intracellular delivery of HCVser by PIDR was enhanced by the addition of anti-HCV antibodies in sera from chronic hepatitis C patients, suggesting that PIDR is an effective reagent for the intracellular delivery of HCVser into the target cells in a receptor-independent manner.

Although direct evidence of enhancement of the adsorption and penetration by the application of spinoculation and polybrene has not been demonstrated yet, sedimentation of the virus particles to the cell surface by the spinoculation and electrostatic interactions between viral particles and cells by the charged polybrene are suggested to overcome the first barrier between virus particles and cells [12–14]. PIDR is a cationic amphiphilic-based protein delivery reagent that forms a complex with proteins through electrostatic and hydrophobic interactions [17]. The complexes of protein molecules and PIDR have been shown to interact with heparan sulfate proteoglycans on the cell surface, and then to be internalized through endocytosis, after which the protein molecules are released from the complexes into the cytoplasm [17], suggesting that PIDR is capable of enhancing not only adsorption but also penetration of HCVser.

Although HCVser are composed of heterogenous viral populations and a large fraction of the viral particles was associated with lipoproteins or neutralizing antibodies [25], these particles are capable of invading into human hepatocytes and establishing a persistent infection *in vivo* [1]. Therefore, it is feasible to speculate that some host factors are involved in the entry of HCVser into hepatocytes *in vivo*. Recently, Stamataki et al. [26] suggested that peripheral blood B lymphocytes participate as a reservoir for HCV for persistent infection and as a vehicle for transinfection to hepatocytes. Although the precise mechanisms of the entry of HCV have not been clarified yet, PIDR is an efficient modality to overcome the obstacles to the entry of HCV.

Recent studies have revealed that at least four cellular molecules play crucial roles in the infection of HCV into hepatocytes *in vitro*: hCD81, scavenger receptor class B type I (SR-BI) [27], and tight junction proteins claudin-1 [28] and occludin [11]. In this study, the entry of HCVser by the treatment with PIDR was shown to be independent from hCD81. Although the involvement of receptor candidates other than hCD81 was not examined in this study, PIDR was shown to enhance the entry of HCVser in cell lines including Huh7, HepG2, HepCD81, Hc and HuS/E2, suggesting that PIDR is capable of enhancing the entry of HCV through a pathway independent from the expression of these receptor candidates.

Previous studies have indicated that HCV infects not only hepatocytes but also lymphoid tissues and peripheral blood mononuclear cells [29], and that the quasispecies nature of viral particles was different among tissues infected with HCV [10]. Furthermore, it was shown that the *in vitro* transcribed JFH-1 RNA used for the recovery of infectious particles contained 2.21×10^{11} copies/μg [30], which is much higher than the amount of viral RNA detected in the patient's sera. The variety of cell tropisms depending on the quasispecies of HCV particles, a low viral load in sera co-existing with neutralization antibodies, and the lack of identified co-factors including functional environment of the liver might be the major obstacles to establishing cell culture systems for the propagation of HCVser. Several approaches have been taken for the establishment of an *in vitro* cell culture system of HCV, including the culture of human liver cells in a three-dimensional radial-flow bioreactor [31], the three-dimensional culture of immortalized primary hepatocytes [7], and the micropatterned culture of primary hepatocytes [8]. These innovative approaches to the cell culture of liver cells, in combination with PIDR which is able to overcome the first barrier of HCV propagation might

contribute to a breakthrough in the establishment of a robust cell culture system of HCVser.

In this study, we demonstrated that PIDR is able to internalize HCV in a receptor-independent manner and provides a clue toward the development of a cell culture system of HCVser in the presence of neutralization antibodies. PIDR may also be useful for the study of viruses that are difficult to internalize into cells due to their low viral titers or the presence of neutralizing antibodies.

Acknowledgments

We thank H. Murase for secretarial work.

This research was supported in part by grants-in-aid from the Ministry of Health, Labor, and Welfare, and the Ministry of Education, Culture, Sports, Science, and Technology, Japan.

References

[1] L.-B. Seeff, Natural history of chronic hepatitis C, Hepatology 36 (2002) S35–S46.

[2] M.-P. Manns, J.-G. McHutchison, S.-C. Gordon, V.-K. Rustgi, M. Shiffman, R. Reindollar, Z.-D. Goodman, K. Koury, M. Ling, J.-K. Albrecht, Peginterferon alfa-2b plus ribavirin compared with interferon alfa-2b plus ribavirin for initial treatment of chronic hepatitis C: a randomised trial, Lancet 358 (2001) 958–965.

[3] J.-M. Pawlotsky, S. Chevaliez, J.-G. McHutchison, The hepatitis C virus life cycle as a target for new antiviral therapies, Gastroenterology 132 (2007) 1979–1998.

[4] T. Wakita, T. Pietschmann, T. Kato, T. Date, M. Miyamoto, Z. Zhao, K. Murthy, A. Habermann, H.-G. Krausslich, M. Mizokami, R. Bartenschlager, T. Jake-Liang, Production of infectious hepatitis C virus in tissue culture from a cloned viral genome, Nat. Med. 11 (2005) 791–796.

[5] N. Hiraga, M. Imamura, M. Tsuge, C. Noguchi, S. Takahashi, E. Iwao, Y. Fujimoto, H. Abe, T. Maekawa, H. Ochi, C. Tateno, K. Yoshizawa, A. Sakai, Y. Sakai, M. Honda, S. Kaneko, T. Wakita, K. Chayama, Infection of human hepatocyte chimeric mouse with genetically engineered hepatitis C virus and its susceptibility to interferon, FEBS Lett. 581 (2007) 1983–1987.

[6] S. Molina, V. Castet, L. Pichard-Garcia, C. Wychowski, E. Meurs, J.-M. Pascussi, C. Sureau, J.-M. Fabre, A. SaCunha, D. Larrey, J. Dubuisson, J. Coste, J. McKeating, P. Maurel, C. Fournier-Wirth, Serum-derived hepatitis C virus infection of primary human hepatocytes is tetraspanin CD81 dependent, J. Virol. 82 (2008) 569–574.

[7] H.-H. Aly, Y. Qi, K. Atsuzawa, N. Usuda, Y. Takada, M. Mizokami, K. Shimotohno, M. Hijikata, Strain-dependent viral dynamics and virus-cell interactions in a novel in vitro system supporting the life cycle of blood-borne hepatitis C virus, Hepatology 50 (2009) 689–696.

[8] A. Ploss, S.-R. Khetani, C.-T. Jones, A.-J. Syder, K. Trehan, V.-A. Gaysinskaya, K. Mu, K. Ritola, C.-M. Rice, S.-N. Bhatia, Persistent hepatitis C virus infection in microscale primary human hepatocyte cultures, Proc. Natl. Acad. Sci. U. S. A 107 (2010) 3141–3145.

[9] D.-R. Burton, Antibodies, viruses and vaccines, Nat. Rev. Immunol. 2 (2002) 706–713.

[10] R. Sobesky, C. Feray, F. Rimlinger, N. Derian, A. Dos Santos, A.-M. Roque-Afonso, D. Samuel, C. Brechot, V. Thiers, Distinct hepatitis C virus core and F protein quasispecies in tumoral and nontumoral hepatocytes isolated via microdissection, Hepatology 46 (2007) 1704–1712.

[11] A. Ploss, M.-J. Evans, V.-A. Gaysinskaya, M. Panis, H. You, Y.-P. de Jong, C.-M. Rice, Human occludin is a hepatitis C virus entry factor required for infection of mouse cells, Nature 457 (2009) 882–886.

[12] N. Landazuri, J.-M. Le Doux, Complexation of retroviruses with charged polymers enhances gene transfer by increasing the rate that viruses are delivered to cells, J. Gene Med. 6 (2004) 1304–1319.

[13] U. O'Doherty, W.-J. Swiggard, M.-H. Malim, Human immunodeficiency virus type 1 spinoculation enhances infection through virus binding, J. Virol. 74 (2000) 10074–10080.

[14] R. Watanabe, S. Matsuyama, F. Taguchi, Receptor-independent infection of murine coronavirus: analysis by spinoculation, J. Virol. 80 (2006) 4901–4908.

[15] L. Ye, X. Wang, S. Wang, G. Luo, Y. Wang, H. Liang, W. Ho, Centrifugal enhancement of hepatitis C virus infection of human hepatocytes, J. Virol. Methods 148 (2008) 161–165.

[16] I. Benedicto, F. Molina-Jimenez, B. Bartosch, F.-L. Cosset, D. Lavillette, J. Prieto, R. Moreno-Otero, A. Valenzuela-Fernandez, R. Aldabe, M. Lopez-Cabrera, The tight junction-associated protein occludin is required for a postbinding step in hepatitis C virus entry and infection, J. Virol. 83 (2009) 8012–8020.

[17] C.-O. Weill, S. Biri, A. Adib, P. Erbacher, A practical approach for intracellular protein delivery, Cytotechnology 56 (2008) 41–48.

[18] T. Okamoto, H. Omori, Y. Kaname, T. Abe, Y. Nishimura, T. Suzuki, T. Miyamura, T. Yoshimori, K. Moriishi, Y. Matsuura, A single-amino-acid mutation in hepatitis C virus NS5A disrupting FKBP8 interaction impairs viral replication, J. Virol. 82 (2008) 3480–3489.

[19] H. Tani, Y. Komoda, E. Matsuo, K. Suzuki, I. Hamamoto, T. Yamashita, K. Moriishi, K. Fujiyama, T. Kanto, N. Hayashi, A. Owsianka, A.-H. Patel, M.-H. Whitt, Y. Matsuura, Replication-competent recombinant vesicular stomatitis virus encoding hepatitis C virus envelope proteins, J. Virol. 81 (2007) 8601–8612.

[20] H.-H. Aly, K. Watashi, M. Hijikata, H. Kaneko, Y. Takada, H. Egawa, S. Uemoto, K. Shimotohno, Serum-derived hepatitis C virus infectivity in interferon regulatory factor-7-suppressed human primary hepatocytes, J. Hepatol. 46 (2007) 26–36.

[21] J. Zhong, P. Gastaminza, G. Cheng, S. Kapadia, T. Kato, D.-R. Burton, S.-F. Wieland, S.-L. Uprichard, T. Wakita, F.-V. Chisari, Robust hepatitis C virus infection in vitro, Proc. Natl. Acad. Sci. U. S. A 102 (2005) 9294–9299.

[22] T. Morris, B. Robertson, M. Gallagher, Rapid reverse transcription-PCR detection of hepatitis C virus RNA in serum by using the TaqMan fluorogenic detection system, J. Clin. Microbiol. 34 (1996) 2933–2936.

[23] R.F. Clayton, A. Owsianska, J. Aitken, S. Graham, D. Bhella, A.H. Patel, Analysis of antigenicity and topology of E2 glycoprotein present on recombinant hepatitis C virus-like particles, J. Virol. 76 (2002) 7672–7682.

[24] P. Pileri, Y. Uematsu, S. Campagnoli, G. Galli, F. Falugi, R. Petracca, A.-J. Weiner, M. Houghton, D. Rosa, G. Grandi, S. Abrignani, Binding of hepatitis C virus to CD81, Science 282 (1998) 938–941.

[25] D. Lavillette, Y. Morice, G. Germanidis, P. Donot, A. Soulier, E. Pagkalos, G. Sakellariou, L. Intrator, B. Bartosch, J.-M. Pawlotsky, F.-L. Cosset, Human serum facilitates hepatitis C virus infection, and neutralizing responses inversely correlate with viral replication kinetics at the acute phase of hepatitis C virus infection, J. Virol. 79 (2005) 6023–6034.

[26] Z. Stamataki, C. Shannon-Lowe, J. Shaw, D. Mutimer, A.-B. Rickinson, J. Gordon, D.-H. Adams, P. Balfe, J.-A. McKeating, Hepatitis C virus association with peripheral blood B lymphocytes potentiates viral infection of liver-derived hepatoma cells, Blood 113 (2009) 585–593.

[27] E. Scarselli, H. Ansuini, R. Cerino, R.-M. Roccasecca, S. Acali, G. Filocamo, C. Traboni, A. Nicosia, R. Cortese, A. Vitelli, The human scavenger receptor class B type I is a novel candidate receptor for the hepatitis C virus, EMBO. J. 21 (2002) 5017–5025.

[28] M.-J. Evans, T. von Hahn, D.-M. Tscherne, A.-J. Syder, M. Panis, B. Wolk, T. Hatziioannou, J.-A. McKeating, P.-D. Bieniasz, C.-M. Rice, Claudin-1 is a hepatitis C virus co-receptor required for a late step in entry, Nature 446 (2007) 801–805.

[29] J.-T. Blackard, N. Kemmer, K.-E. Sherman, Extrahepatic replication of HCV: insights into clinical manifestations and biological consequences, Hepatology 44 (2006) 15–22.

[30] T. Kato, T. Date, M. Miyamoto, A. Furusaka, K. Tokushige, M. Mizokami, T. Wakita, Efficient replication of the genotype 2a hepatitis C virus subgenomic replicon, Gastroenterology 125 (2003) 1808–1817.

[31] H. Aizaki, S. Nagamori, M. Matsuda, H. Kawakami, O. Hashimoto, H. Ishiko, M. Kawada, T. Matsuura, S. Hasumura, Y. Matsuura, T. Suzuki, T. Miyamura, Production and release of infectious hepatitis C virus from human liver cell cultures in the three-dimensional radial-flow bioreactor, Virology 314 (2003) 16–25.

Virus Research xxx (2011) xxx–xxx

Contents lists available at ScienceDirect

Virus Research

journal homepage: www.elsevier.com/locate/virusres

Review

Structure of hepatitis E viral particle

Yoshio Mori[a,b], Yoshiharu Matsuura[a,*]

[a] Department of Molecular Virology, Research Institute for Microbial Diseases, Osaka University, 3-1 Yamada-oka, Suita, Osaka 565-0871, Japan
[b] Department of Virology III, National Institute of Infectious Diseases, Tokyo, Japan

ARTICLE INFO

Article history:
Available online xxx

Keywords:
Hepatitis E virus
Capsid protein
Crystal structure
Particle assembly

ABSTRACT

Hepatitis E is acute hepatitis caused by infection of hepatitis E virus (HEV) via a fecal-to-oral or zoonotic route. HEV is a small, non-enveloped virus containing positive strand RNA as a genome. Recently, the three-dimensional structures of the HEV-like particles and spike domain protruded from the surface of the particle expressed by recombinant baculovirus or bacteria have been revealed. Based on these reports, the structural features of the HEV capsid subunit and viral particle are reviewed to give insights to the mechanisms underlying the particle assembly, antigenicity, host cell attachment and native virion packaging.

Contents

1. Introduction

Earlier studies using immuno-electron microscopy revealed that hepatitis E virus (HEV) obtained from human fecal specimens was a nonenveloped icosahedral particle with indentations on the surface (Balayan et al., 1983; Bradley et al., 1988; Sreenivasan et al., 1984). Particles purified by sucrose gradient centrifugation had a diameter of 320–340 Å (Bradley et al., 1988). Based on observation by electron microscopy, the morphology of HEV was similar to those of "small round viruses" in feces samples, such as Norwalk virus (the family *caliciviridae*) and hepatitis A virus (the family *picornaviridae*). Like other hepatitis viruses, HEV could not efficiently replicate in cell culture until recently. Therefore, almost of detailed structural analyses regarding HEV particles relied upon recombinant proteins by baculoviral or bacterial expression system.

HEV is the sole member of the genus *hepevirus* within the family *hepeviridae* (Panda et al., 2007). This virus has a single, positive-stranded RNA genome of 7.2 kb in length, which is capped with m7G and polyadenylated at the 5′- and 3′-termini, respectively (Okamoto, 2007). The genome contains three open reading frames (ORF), ORF1, ORF2 and ORF3. The viral capsid protein encoded by ORF2 works for particle assembly, binding to host cells, and eliciting of neutralizing antibodies. Expression of truncated capsid protein in insect cells by baculovirus expression system resulted in self-assembly of the capsid protein and production of two types of HEV-like particle (HEV-LP) with different diameters (Li et al., 1997, 2005, 2007; Xing et al., 2010). In this review, the small and large HEV-LPs were designated as HEV-LP/$T=1$ and HEV-LP/$T=3$, respectively, based on difference of packaging of the capsid protein

Abbreviations: HEV, hepatitis E virus; HEV-LP, HEV-like particle; HSPGs, heparan sulfate proteoglycans; NOB, neutralizing-of-binding; ORF, open reading frame.

* Corresponding author. Tel.: +81 6 6879 8340; fax: +81 6 6879 8269.
E-mail address: matsuura@biken.osaka-u.ac.jp (Y. Matsuura).

0168-1702/$ – see front matter © 2011 Published by Elsevier B.V.
doi:10.1016/j.virusres.2011.03.015

Please cite this article in press as: Mori, Y., Matsuura, Y., Structure of hepatitis E viral particle. Virus Res. (2011), doi:10.1016/j.virusres.2011.03.015

Table 1
Structural properties of HEV-LPs and HEV virion.

	HEV-LP/$T=1$	HEV-LP/$T=3$	HEV virion
Diameter	270 Å[a]	410 Å[b]	320–340 Å[c]
Amino acid residues forming particle	ORF2 aa126–601 (as a minimum requirement)[d]	ORF2 aa112–608?[b]	ORF2 aa1–660?
Number of capsid subunit	60[a]	180[b]	180?
Triangulation number	$T=1$[a]	$T=3$[b]	$T=3$?
RNA packaging	No[a]	Yes[b]	Yes

[a] Xing et al. (1999).
[b] Xing et al. (2010).
[c] Bradley et al. (1988).
[d] Li et al. (2005).

(Table 1 and see below). The structural analyses of HEV-LP/$T=1$ preceded those of HEV/$T=3$ because of simplicity of purification of the former from the cell supernatant. In the first structural study using a low-resolution (22 Å) cryoelectron microscopy, it was shown that the genotype 1 HEV-LP/$T=1$ formed $T=1$ icosahedral particle composed of 60 copies of the truncated capsid protein (Xing et al., 1999). HEV-LP/$T=1$ appeared to be empty due to no significant density of RNA inside and exhibited 270 Å in diameter, which is less than the diameter of partially purified native virions. However, HEV-LP/$T=1$ displayed similar properties to the native HEV particles in terms of antigenicity and surface substructure (Li et al., 2004; Xing et al., 1999). Thus, HEV-LP/$T=1$ is thought to be a good material to approach a three-dimensional structure of the native HEV. Until now, three laboratories, including us, succeeded to resolve the crystal structures of HEV-LP/$T=1$ of genotypes 1 (Xing et al., 2010), 3 (Yamashita et al., 2009) and 4 (Guu et al., 2009). Meanwhile, a cryoelectron microscope structure of HEV-LP/$T=3$ has been reported very recently (Xing et al., 2010), suggesting the more plausible packaging of the HEV virion. In addition, another study using a bacteria expression system illustrated the more detailed structure of the protruding spike domain of HEV (Li et al., 2009). Here, the accumulating information from mainly these reports is reviewed to understand the structural basis regarding the particle assembly, antigenicity, host cell binding and the native virion packaging.

2. Primary structure of the HEV capsid protein

ORF2 encodes the major capsid protein composed of 660 amino acid residues (Fig. 1). Among four major mammalian HEV genotypes, genetic homology of amino acid residues of the capsid

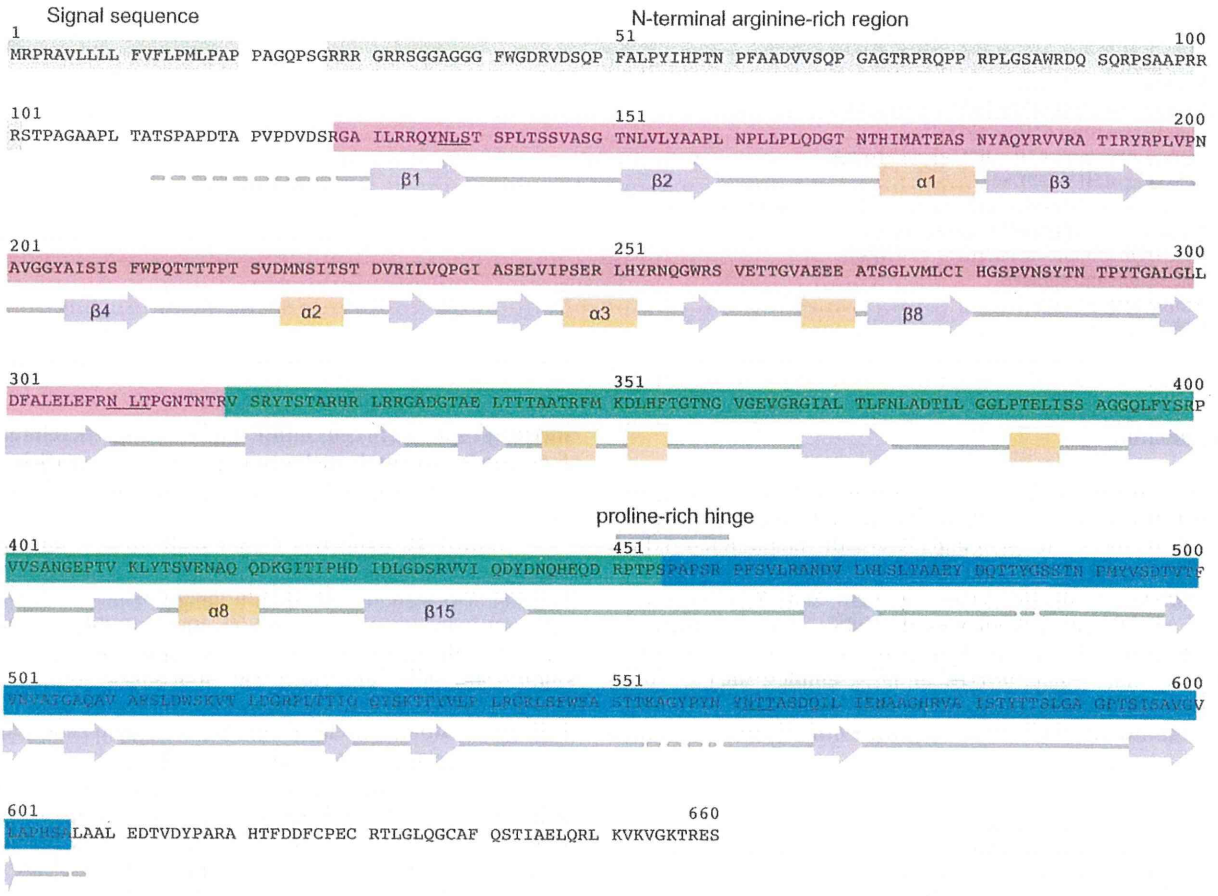

Fig. 1. Secondary structure assignment of the capsid protein of HEV-LP. It is represented based on the data from the crystal structure of HEV-LP of the genotype 3 2712 strain (PDB ID, 2ZTN). The truncated form of the amino acid residues 112–608 is used for production of HEV-LP. The S, M and P domains are shown in pink, green and blue, respectively. α-Helices, β-sheets and loops are indicated as orange rectangles, purple arrows and thick lines, respectively. Disorder regions are shown by dotted lines.

Please cite this article in press as: Mori, Y., Matsuura, Y., Structure of hepatitis E viral particle. Virus Res. (2011), doi:10.1016/j.virusres.2011.03.015

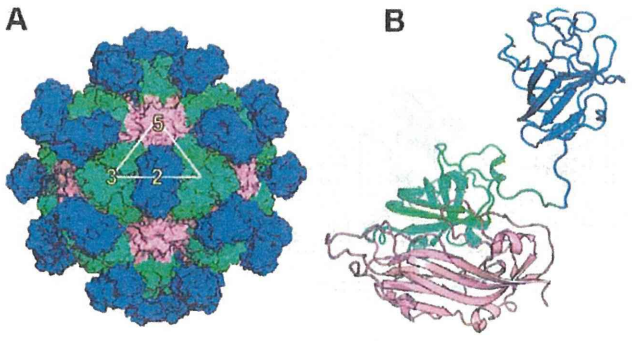

Fig. 2. Crystal structures of HEV-LP (A) and the capsid protein monomer (B). The S, M and P domains are shown in pink, green and blue, respectively. (A) The surface diagram of HEV-LP. Representatives of 2-, 3- and 5-fold icosahedral axes are indicated.

protein was over 85% (data not shown). Many of amino acid divergences were found in the N-terminal 111 amino acids residues. Compared to other nonenvelope viruses, it is notable that the HEV capsid protein has a property of general secreted proteins, which contain a signal sequence at the N-terminus and N-linked glycosylation sites (three asparagine residues 137, 310, 562) (Fig. 1). Although the capsid protein expressed in mammalian cells was detected as 74 kDa unglycosylated and 88 kDa glycosylated forms (Jameel et al., 1996), it is controversial which forms (or both) build the virion. The N-terminal domain followed by the signal sequence (residues 28–101) is an arginine-rich domain resemble to an RNA-binding domain of the coat proteins of tombusviruses. In insect cells, the HEV capsid protein was proteolytically cleaved, resulting in yields of several polypeptides with various molecular weights (Li et al., 1997). The 53 kDa-truncated form, which lacked the signal sequence, N-terminal arginine-rich and C-terminal domains, was able to self-assemble to the HEV-LP/$T=1$ in the supernatant of insect Tn5 cells. Minimum requirement for assembly of HEV-LP/$T=1$ were amino acid residues 126–601(Li et al., 2005). Another truncated form of 64 kDa was highly associated with cells, but it was also self-assembled to HEV-LP/$T=3$ (Li et al., 2007; Xing et al., 2010). The precise amino acid residues consisting the 64 kDa capsid protein are not known. However, the N-terminal domain followed by the putative signal sequence was required for HEV-LP/$T=3$ formation because it was detected upon expression of the capsid protein including amino acids 14–608, but not 112–608 (data not shown).

3. Overall structure of HEV-LP/$T=1$

The crystal structures of HEV-LP/$T=1$ derived from the genotypes 1 (PDB ID; 2ZZQ), 3 (PDB ID; 2ZTN) and 4 (PDB ID; 3HAG) were resolved at the resolution of amino acid level (3.5–3.8 Å) (Guu et al., 2009; Xing et al., 2010; Yamashita et al., 2009). These structures were almost identical in spite of some divergence of amino acid residues (Xing et al., 2010). HEV-LP/$T=1$ showed a $T=1$ symmetry with an internal diameter of approximately 125 Å and an external diameter of approximately 270 Å. The particles are composed of 60 subunits of the truncated capsid proteins, and icosahedral 2-, 3- and 5-fold axes were found in the particle (Fig. 2A). The pronounced structural feature is 30 dimeric protruding spikes of 30 Å in length at the surface of the 2-fold axes. Board depressions are located around the 5-fold axis.

4. Tertiary structure of the HEV capsid protein

The crystal structures of the capsid monomer building HEV-LP/$T=1$ showed that they could be divided into three domains designated as S (shell), M (middle) and P (protruding) (Xing et al., 2010; Yamashita et al., 2009) (Figs. 1 and 2). In the report by Guu et al. (2009), the M and P domains were designated as the P1 and P2 domains, respectively, according to the finding of moderate protrusions formed by the M domain over the internal shell of the particle. These domains are composed of 128–319, 320–455 and 456–606, respectively, in the case of the genotype 3 HEV-LP/$T=1$ (Yamashita et al., 2009). All of the three domains fold to β-barrel structures by anti-parallel β-sheets (Figs. 1 and 2B). The S domain displays a typical jerry roll-like β-barrel fold as observed in various $T=3$ viral capsid proteins. Interestingly, a structural homolog search revealed that the HEV S domain is more related to the jerry-roll domains of coat proteins of members of the genera *tombusviruses* and *sobemoviruses*, which are plant small round viruses with a $T=3$ symmetry, than those of any animal viruses (Guu et al., 2009). Among animal viruses, the domain of the Norwalk virus capsid protein, which was thought to be originally related to that of HEV, exhibited much less homology than that of Seneca Valley virus, an oncolytic picornaviruses (Guu et al., 2009).

The other domains, M and P, represent very remarkable structure compared with viral capsid proteins that have been ever reported (Fig. 2B). The M domain is tightly associated with the S domain and locates at the surface around the 3-fold axis of the particle. The related domains were not found among the small round viruses with a $T=3$ symmetry with the structural similarity (Guu et al., 2009). The P domain dimer forms the protruding spike around the 2-fold axis of HEV-LP/$T=1$ as well as those of the caliciviruses and the plant tombusviruses. However, the HEV P domain also does not share significant structural homology with any other viral proteins (Guu et al., 2009). The P domain of the caliciviruses could divide into two subdomains, P1 and P2 (Chen et al., 2006; Prasad et al., 1999), while the HEV P domain is composed of a single domain. The size of HEV P domain is roughly half of those of the caliciviruses. Furthermore, the P dimer of HEV indicates a crossing topology of the P versus M and S domains while those of the caliciviruses do a parallel topology (Yamashita et al., 2009) (Fig. 3A). The flexibility of a long proline-rich hinge region linked between the M and P domains (amino acid residues 445–467) allows this unique topology of HEV-LP/$T=1$. In addition, the hinge also contributes to topological change of the protruding spike in HEV-LP/$T=3$ (see below) (Xing et al., 2010).

Approximately 10 amino acid residues at the N-terminus of the truncated capsid proteins building HEV-LP/$T=1$ (amino acid residues 118–127) of the genotypes 1 and 4 were resolved to be as the extended arm domain (Guu et al., 2009; Xing et al., 2010), of which related domain was found in the coat protein of tombusvirus. The extended loop interacts the adjacent capsid subunit, contributing formation of the capsid protein dimer of HEV-LP/$T=1$.

5. Packaging of HEV-LP/$T=1$

Three different interactions of capsid subunits are required for packaging of HEV-LP/$T=1$; briefly dimeric, trimeric and pentameric interactions around 2-, 3- and 5-fold icosahedral axes, respectively. The three domains, S, M and P, play different roles of the packaging of HEV-LP/$T=1$. The S domain is involved in all the interactions and builds the integral shell by itself. The inner surface of the shell is rich in basic amino acids (6 arginine residues per one subunit) (Guu et al., 2009). This cluster of arginine residues may contribute to neutralize negative charges of the genomic RNA. The M domain located around the 3-fold axis and is involved in trimeric interaction (Fig. 3B). The domain also interacts with the P domain of counterpart, contributing to the dimeric interaction to some extent (Yamashita et al., 2009). The P domain works only dimeric interaction. It was reported that the P domain expressed alone formed a strong dimer (Li et al., 2009). The tight interaction is

Please cite this article in press as: Mori, Y., Matsuura, Y., Structure of hepatitis E viral particle. Virus Res. (2011), doi:10.1016/j.virusres.2011.03.015

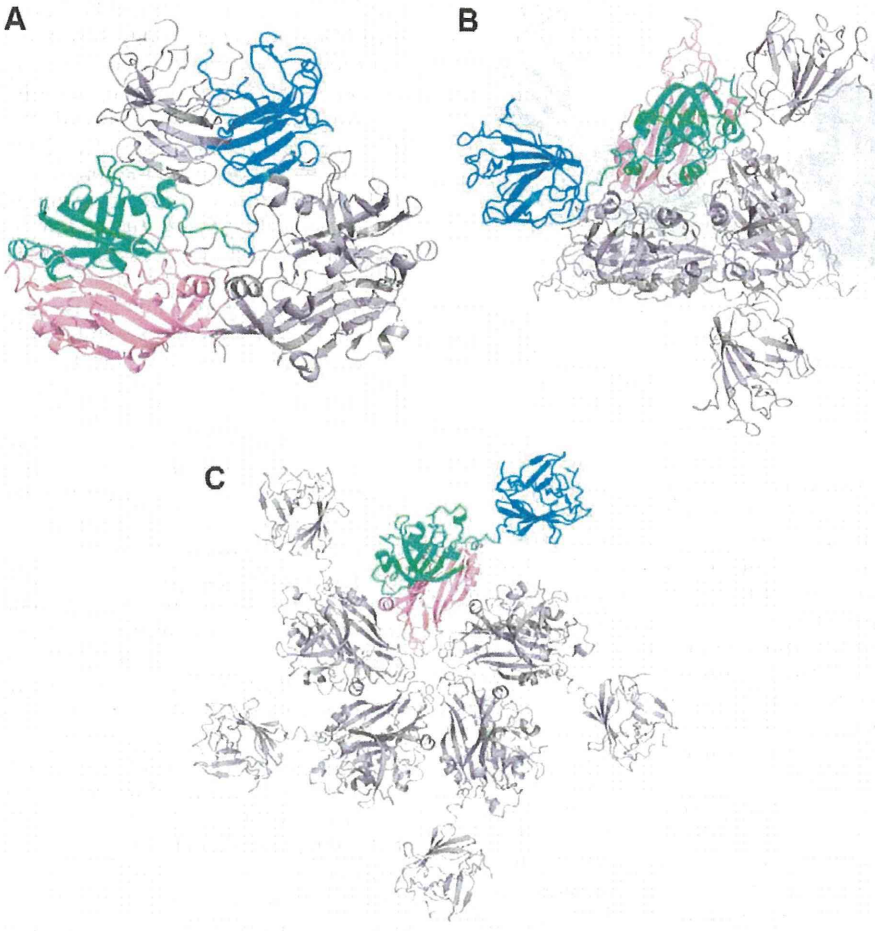

Fig. 3. Packagings of dimer, trimer and pentamer at 2-, 3- and 5-fold icosahedral axes, respectively. The side view of the dimer (A) and the views from outside of the trimer (B) and pentamer (C) are illustrated. The S, M and P domains of one monomer are shown in pink, green and blue, respectively.

mediated by a hydrophobic cluster of the dimer interface (Li et al., 2009).

The surface areas buried by the dimeric, trimeric and pentameric interactions were approximately 5300–5900 Å^2, 3000–3400 Å^2 and 1400–1600 Å^2, respectively, suggesting that the pentameric formation could limit rate of particle assembly (Guu et al., 2009; Xing et al., 2010). Notably, the center of the pentamer structure is thinnest in the particle (Yamashita et al., 2009) (Fig. 3C). The mutagenesis analysis revealed that Tyr288 in the center of the pentamer was crucial for the particle formation (Yamashita et al., 2009). Aromatic amino acids (phenylalanine and tryptophan) were replaceable to Tyr288 in terms of the particle formation. This residue is completely conserved in major mammalian and avian genotypes of HEV (Yamashita et al., 2009). Meanwhile, the other aromatic residues were found in the corresponding position of the novel HEV found in wild rats (Johne et al., 2010) and the structurally related caliciviruses and tombusviruses (Yamashita et al., 2009). This suggests that the aromatic amino acid residues in the center of 5-fold axis are functionally conserved during the evolutional process.

Based on the width of the interaction area, it is hypothesized that the packaging of HEV proceeds in the sequence of dimeric, trimeric, and pentameric formation. Xing et al. (2010) attempted to evaluate the packaging sequence using an *in vitro* reassembly assay of the capsid proteins disassembled from HEV-LP/T=3 by a combination of chelating and reduced reagents. As a result, decamer complexes (pentamers of dimer), but not hexamers (trimers of dimer), were observed in the assay, suggesting that the pentamer formation is more preferentially occurred than the trimer formation via not only simple protein–protein interactions.

6. Cell-attachment region and antigenic sites of neutralizing antibodies

It was reported that HEV-LP/T=1 bond to cell surface via heparan sulfate proteoglycans (HSPGs), and HSPGs were required for HEV infection in culture cells (Kalia et al., 2009). In the cases of Norwalk virus and feline calicivirus, the apical surface of the protruding spike was involved in binding to the receptor molecules, histo-blood antigens (Bu et al., 2008; Choi et al., 2008) and feline junctional adhesion molecule (Bhella et al., 2008), respectively. In order to determine crucial amino acid residues for cell-binding, we examined the cell-attachment activity of a series of HEV-LP/T=1 with double or single substitutions in amino acid residues at the surface of the P domain in the previous study (Yamashita et al., 2009). The result showed that the double substitutions, T489A and P491A, N560A and Y561A, N562A and T564A, or T585A and T586A, resulted in lack of attachment activity of HEV-LP/T=1 to Huh7 and A549 cells, which were known to be susceptive to HEV infection (Fig. 4A). These residues were mapped in the exposed loops of the apical center region of the protruding spike, suggesting that this region is involved in binding to receptor molecules such as HSPGs. The data suggesting that the dimer formation of HEV capsid protein was prerequisite for the receptor-binding (He et al., 2008) would support the involvement of the apical surface near the dimeric interacting domain of the P dimer in cell-attachment.

Please cite this article in press as: Mori, Y., Matsuura, Y., Structure of hepatitis E viral particle. Virus Res. (2011), doi:10.1016/j.virusres.2011.03.015